Partial Channel Quality Information Feedback in Multiuser Relay Networks Over Nakagami-*m* Fading

Yao Lu, Nan Yang, *Member, IEEE*, Maged Elkashlan, *Member, IEEE*, and Jinhong Yuan, *Senior Member, IEEE*

***Abstract*—We propose a new partial feedback scheme in multiuser relay networks (MRNs) where a source communicates with K destinations via a relay. We focus on a practical network model where orthogonal frequency division multiple access (OFDMA) is adopted in the downlink and only limited feedback overhead is supported in the uplink. For this model, we consider that the OFDMA spectrum consists of M_{RB} resource blocks (RBs). In the proposed scheme, the destinations feed back the channel quality information (CQI) for the best M_{FB} RBs, instead of all M_{RB} RBs, to the source through the relay, which fulfills the requirement of feedback overhead. Considering the highly versatile Nakagami-*m* fading, we derive new closed-form expressions for the exact sum rate for ideal CQI feedback and quantized CQI feedback. We also derive the asymptotic sum rate expression for ideal CQI feedback. We have some new findings to understand the impact of network and channel parameters on the sum rate. First, a more scattering fading environment with a lower m decreases the sum rate for a small K, but increases the sum rate for a large K. Second, the sum rate increases as M_{FB} approaches M_{RB}. Third, the sum rate gap between ideal CQI feedback and quantized CQI feedback increases when M_{FB} or K increases. Fourth, we demonstrate that the proposed partial feedback scheme achieves almost the same sum rate as the full feedback scheme for a large number of destinations.**

***Index Terms*—Multiuser relay network, partial channel quality information feedback, opportunistic scheduling, orthogonal frequency division multiplex access, Nakagami-*m* fading.**

I. Introduction

OPPORTUNISTIC scheduling has emerged as an effective strategy for radio resource management that exploits the inherent diversity in multiuser networks, especially when the number of users is large [1], [2]. The basic idea of opportunistic scheduling is to schedule a user with the highest channel quality, thus improving the throughput of the network [3]. Due to its benefits, opportunistic scheduling has been applied in some established standards, e.g., Qualcomms high data rate (HDR) [4] and high-speed downlink packet access (HSDPA) [5]. Despite of its success in practical applications, it is widely agreed that opportunistic scheduling relies heavily on the feedback of precise channel estimates, which apparently incurs a substantial burden of feedback overhead. Importantly, this burden becomes overwhelming in orthogonal frequency-division multiple access (OFDMA) systems, since feedback for all the blocks of sub-carriers may easily overwhelm the feedback link, even for a system with a small number of users. In an OFDMA system with K users, for example, sub-carriers are grouped into M_{RB} resource blocks (RBs) and each RB is used as a scheduling unit. As a result, the number of the CQIs required by the scheduler is KM_{RB}, which causes a high feedback overhead in the uplink. To reduce the feedback overhead, numerous research efforts have been devoted into designing schemes with low feedback overhead [6]–[16]. One effective scheme is opportunistic feedback which selects the users with the highest scheduling probability to feed back their CQI to the source [6]–[9]. Another scheme is partial feedback (e.g., best-M in Long-Term Evolution (LTE) systems), which allows each user to feed back the best M_{FB} CQI values out of M_{RB} to the source [10]–[16].

Recently, the adoption of OFDMA in multiuser relay networks (MRNs) has received considerable attention in practical applications, such as the LTE-Advanced (LTE-A) system [17], [18] and the Mobile Worldwide Interoperability for Microwave Access (WiMAX) system [19], [20]. This adoption has posed new challenges to the design of scheduling and feedback schemes, since the CQIs of both the source-relay link and the relay-user link are required for the scheduler to assign resources. Against this background, some scheduling schemes have been studied for relay networks [21]–[25]. In [21] and [22], the sum-rate was maximized under the constraint that the relay has the same receiving rate and transmission rate. A generalized proportional fairness was addressed in [23] for OFDMA amplify-and-forward (AF) relay networks. In [24], the resource allocation and user scheduling were optimized for the shared relay system under the practical wireless backhaul constraint. In [25], a joint user-and-hop scheduling strategy was proposed to reap the benefits of multiuser diversity and multi-hop diversity together. We note that all of these studies are based on an ideal assumption that the channel state information of all links is completely known at the scheduler. Needless to say, this requires a huge amount of resources in the feedback link for practical implementation. Therefore, an overhead reduction is required in the feedback link to balance the scheduling performance with limited resources in MRNs.

Manuscript received August 5, 2014; revised January 19, 2015; accepted April 19, 2015. Date of publication April 24, 2015; date of current version September 7, 2015. The work of J. Yuan was supported by the Australian Research Council Discovery Project (DP120102607). The associate editor coordinating the review of this paper and approving it for publication was A. Kwasinski.

Y. Lu is with the China Information Technology Designing and Consulting Institute, China Unicom, Beijing 100048, China (e-mail: idboom@gmail.com).

N. Yang is with the Research School of Engineering, Australian National University, Canberra, ACT 0200, Australia (e-mail: nan.yang@anu.edu.au).

M. Elkashlan is with the School of Electronic Engineering and Computer Science, Queen Mary University of London, E1 4NS London, U.K. (e-mail: maged.elkashlan@qmul.ac.uk).

J. Yuan is with the School of Electrical Engineering and Telecommunications, University of New South Wales, Sydney, NSW 2052, Australia (e-mail: j.yuan@unsw.edu.au).

Digital Object Identifier 10.1109/TWC.2015.2426175

In this paper, we propose a new partial feedback scheme in MRNs where the communication between the source and the K destinations is assisted by a decode-and-forward (DF) relay. We consider that OFDMA is employed in the downlink and the OFDMA spectrum is assumed to provide M_{RB} RBs. In the network, opportunistic scheduling is adopted among multiple destinations such that the destination with the highest end-to-end CQI is selected for transmission. To reduce the feedback overhead incurred by opportunistic scheduling, our proposed scheme utilizes the best M_{FB} RBs to convey the CQI from the destinations to the source via the relay. To allow the source to know the equivalent end-to-end CQI of the source-relay-destination link, our proposed scheme requires the relay to calculate the equivalent end-to-end CQI and then feed it back along with the corresponding RB indices and destination indices to the source. To examine the performance achieved by our proposed scheme, we derive new closed-form expressions for the exact sum rate in practical Nakagami-m fading channels for two cases, namely, ideal CQI feedback and quantized CQI feedback. To this end, new exact expressions are derived for the cumulative distribution function (CDF) of the highest end-to-end SNR associated with the scheduled destination. We also derive an asymptotic sum rate expression for ideal CQI feedback, which accurately predicts the network performance for a large number of destinations. We further derive an approximate expression that characterizes the sum rate gap between ideal CQI feedback and quantized CQI feedback, based on which the impact of network parameters on this gap is examined. Using these results, we provide some new findings that allow us to understand the impact of network and channel parameters on the sum rate, as follows.

1) We find that a more scattering environment with a lower Nakagami-m fading parameter m reduces the sum rate for a small K, but improves the sum rate for a large K. This finding is due to the fact that when m decreases, the fading environment becomes more scattering and the received signals become more fluctuated. The higher signal fluctuation together with a larger number of users enables the scheduler to arrange transmissions at higher peaks of channel fading, which leads to an improved sum rate.
2) We find that an increasing M_{RB} with a fixed M_{FB} reduces the sum rate. We also find that an increasing M_{FB} with a fixed M_{RB} improves the sum rate. These findings are due to the fact that the sum rate is an increasing function of a factor $\left[1-\left(1-\frac{M_{\mathrm{FB}}}{M_{\mathrm{RB}}}\right)^{K}\right]$. When M_{RB} increases, the factor decreases, leading to a reduced sum rate. When M_{FB} increases, the factor increases, leading to an improved sum rate.
3) We find that the sum rate gap between ideal CQI feedback and quantized CQI feedback decreases as the quantization levels L increases. This finding is due to the fact that an increasing L improves the accuracy of quantized CQIs and lowers the level of quantization noise. We also find that this gap increases as K or M_{FB} increases. This finding is due to the fact that a larger K or M_{FB} increases the number of quantized CQIs and thus raises the level of quantization noise.

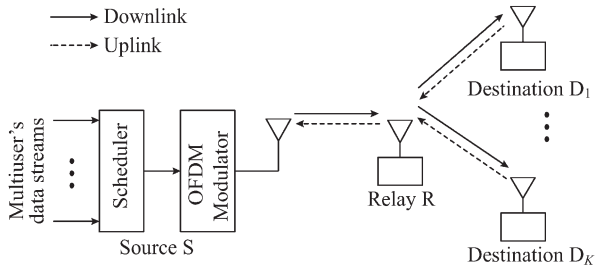

Fig. 1. The schematic illustration of the MRN.

4) We find that the sum rate of our proposed partial feedback scheme asymptotically approaches that of the full feedback scheme which uses all the M_{RB} RBs, as K increases. This finding is due to the fact that the scheduling outage probability for the partial feedback scheme approaches 0 as K grows large and that scheduling outage does not occur in the full feedback scheme.

The rest of this paper is organized as follows. Section II describes the system model and the proposed partial CQI feedback scheme. Section III derives new expressions for the sum rate of ideal and quantized CQI feedback in Nakagami-m fading. Section IV presents numerical and simulation results to examine the impact of network and channel parameters on the performance. Conclusions are finally drawn in Section V.

II. Proposed Partial CQI Feedback Scheme in Multiuser Relay Networks

A. Multiuser Relay Networks

We consider the MRN where the communication between a source S and K destinations $\{\mathrm{D}_k\}_{k=1}^{K}$ is aided by a relay R, as depicted in Fig. 1. In this network, S, R, and $\{\mathrm{D}_k\}_{k=1}^{K}$ can be considered as the base station, the relay station, and the mobile users, respectively. The direct links between the source and the destinations are assumed to be in absence. As such, the communication between S and D_k is performed via R only. This assumption is common in realistic scenarios where the destinations are located a fairly long distance from the source, e.g., at the cell edge or within heavily shadowed areas. We clarify that the MRN without the direct link has been viewed as a typical scenario in the LTE-A system [17], [18] and the WiMAX system [19], [20]. As such, it has been examined in several publications [26]–[29].

In the MRN, we consider the deployment of OFDMA in the downlink such that both S and R transmit data using OFDMA. The aim of this deployment is to subdivide the downlink bandwidth into M_{RB} resource blocks of sub-carriers. Notably, the sub-carrier frequencies are carefully chosen to ensure that the sub-carriers are orthogonal to each other. Therefore, the use of OFDMA enables S to separate the transmissions to multiple users through R and reap the benefits of opportunistic scheduling. We assume that the number of RBs at S is equal to the number of RBs at R, which is denoted by M_{RB}. We also assume that the channel between S and R and the channel between R and D_k are subject to independent frequency-flat fading, where the channels remain unchanged during one end-to-end transmission interval, but change independently between two transmission intervals. Prior to the transmission, R uses the pilot

sub-carriers from S to measure the CQI values on the RBs in the S–R link. Also, D_k uses the pilot sub-carriers from R to measure the CQI values on the RBs in the R–D_k link. Then, D_k feeds back the CQIs together with their RB indices and destination index k to R. Finally, R calculates the equivalent CQI values on the RBs in the S–R–D_k link, and feeds back the CQI values along with their RB indices and destination index k to S.

We assume that R is constrained to a half-duplex operation and adopts the DF relaying protocol to regenerate the data received from S. As such, the downlink transmission from S to D_k is completed within two time slots. In the first time slot, the received signal $y_{R,b}$ at R on RB b is given by

$$y_R, b = \sqrt{P_S d_{S,R}^{-\eta}} h_{R,b} x_b + v_{R,b}, \tag{1}$$

where P_S denotes the transmit power at S, $d_{S,R}$ denotes the distance between S and R, η denotes the path loss exponent, $h_{R,b}$ denotes the channel fading coefficient of S–R link on RB b, x_b denotes the transmitted data on RB b, and $v_{R,b}$ denotes the additive white Gaussian noise (AWGN) component with variance σ^2 at R on RB b. In the second time slot, R decodes the received signal from S. In the case of successful decoding, R re-encodes and retransmits the signal to D_k. Let $\tilde{x}_b$ denote the re-encoded version of x_b at R. The received signal $y_{D_k,b}$ at D_k on RB b is given by

$$y_{D_k,b} = \sqrt{P_R d_{R,D_k}^{-\eta}} h_{D_k,b} \tilde{x}_b + v_{D_k,b}, \tag{2}$$

where P_R denotes the transmit power at R, d_{R,D_k} denotes the distance between R and D_k, $h_{D_k,b}$ denotes the channel fading coefficient of R–D_k link on RB b, and $v_{D_k,b}$ is the AWGN component with variance σ^2 at D_k on RB b. According to (1) and (2), the instantaneous SNRs at R and D_k on RB b are given by $\gamma_{R,b} = |h_{R,b}|^2 d_{S,R}^{-\eta} \rho_S$ and $\gamma_{D_k,b} = |h_{D_k,b}|^2 d_{R,D_k}^{-\eta} \rho_R$, respectively, where $\rho_S = P_S/\sigma^2$ and $\rho_R = P_R/\sigma^2$ denote the transmit SNR at S and R, respectively.[1] Additionally, the average SNRs at R and D_k on RB b are defined as $\bar{\gamma}_{R,b} = \mathbb{E}[\gamma_{R,b}]$ and $\bar{\gamma}_{D_k,b} = \mathbb{E}[\gamma_{D_k,b}]$, respectively, with $\mathbb{E}[\cdot]$ denoting the expectation operation.

In this network, we focus on generalized and versatile Nakagami-m fading channels. The Nakagami fading stands for a wide range of multipath channels via the variation of m [30], [31]. For instance, the Nakagami-m distribution includes the Rayleigh fading ($m = 1$) as a special case. Moreover, when $m > 1$, a one-to-one mapping between the Rician factor and the Nakagami fading parameter allows the Nakagami-m distribution to closely approximate the Rice distribution [31]. More importantly, the Nakagami-m fading often gives the best fit to urban [31] and indoor multipath propagation [32], which are the typical scenarios for relay networks. Here, we denote m_0 as the fading parameter between S and R and denote m_k as the fading parameter between R and D_k. Specifically, we assume independent and identically distributed (i.i.d.) fading among M_{RB} RBs for each destination, which corresponds to a block fading model in the frequency domain [10]. Importantly, the simulation provided in [11] has proved that this assumption is approximately valid for a wide bandwidth OFDMA system. Although this assumption may not be true in every practical system, it indeed enables analytical tractability and provides an upper bound on the capacity of the systems where this assumption does not apply [12]. Based on the i.i.d. distribution across the RBs for each node, the average SNR at R is written as $\mathbb{E}[\gamma_{R,1}] = \mathbb{E}[\gamma_{R,2}] = \cdots = \mathbb{E}[\gamma_{R,M_{RB}}] = \overline{\gamma}_0$ and the average SNR at D_k is written as $\mathbb{E}[\gamma_{D_k,1}] = \mathbb{E}[\gamma_{D_k,2}] = \cdots = \mathbb{E}[\gamma_{D_k,M_{RB}}] = \overline{\gamma}_k$. To alleviate the notation, we define $h_{0,b} \triangleq h_{R,b}$, $h_{k,b} \triangleq h_{D_k,b}$, $\gamma_{0,b} \triangleq \gamma_{R,b}$, and $\gamma_{k,b} \triangleq \gamma_{D_k,b}$, $\forall\, k, b$. As such, the probability density function (PDF) of $\gamma_{u,b}$, $u = 0, 1, \cdots, K$, is given by

$$f_{\gamma_{u,b}}(\gamma) = \frac{1}{\Gamma(m_i)} \left(\frac{m_i}{\overline{\gamma}_u}\right)^{m_i} \gamma^{m_i - 1} e^{-\frac{m_i \gamma}{\overline{\gamma}_u}}, \tag{3}$$

where $i = 0$ for $u = 0$, $i = u$ for $u = 1, 2, \cdots, K$, and $\Gamma(\cdot)$ is the gamma function [33, Eq. (8.310.1)] defined as $\Gamma(x) = (x-1)!$ for integer values of x. We note that Nakagami-m describes a wide range of fading situations by varying m_i. For instance, $m_i = 1$ corresponds to the Rayleigh fading, $m_i > 1$ corresponds to the situation where a specular component coexist with diffuse components, and Nakagami-m approaches additive white Gaussian noise (AWGN) fading when $m \to \infty$. We further denote $X \sim \mathcal{G}(\alpha, \beta)$ as a Gamma distributed random variable with parameters α and β. Therefore, the PDF of X is given by [34]

$$f_X(x) = \frac{\beta^\alpha}{\Gamma(\alpha)} x^{\alpha-1} e^{-\beta x}, \tag{4}$$

and the cumulative distribution function (CDF) of X is given by [34]

$$F_X(x) = \tilde{\Gamma}(\alpha, \beta x), \tag{5}$$

where $\tilde{\Gamma}(\cdot, \cdot)$ is the incomplete Gamma function [33, Eq. (8.350.1)] defined as $\tilde{\Gamma}(a, x) = \int_0^x t^{a-1} e^{-t} dt$. According to (3) and (4), we have $\gamma_{0,b} \sim \mathcal{G}(m_0, \beta_0)$, and $\gamma_{k,b} \sim \mathcal{G}(m_k, \beta_k)$ with $\beta_0 = m_0/\overline{\gamma}_0$ and $\beta_k = m_k/\overline{\gamma}_k$.

We now present the instantaneous SNR at D_k and its statistical properties. If D_k receives the transmitted signal from R on RB b, the equivalent end-to-end instantaneous SNR on RB b, $\tilde{\gamma}_{k,b}$, is given by [35].

$$\tilde{\gamma}_{k,b} = \min\{\gamma_{0,b}, \gamma_{k,b}\}. \tag{6}$$

Otherwise, we have $\tilde{\gamma}_{k,b} = 0$. Based on the results of order statistics [36], we derive the CDF of $\tilde{\gamma}_{k,b}$, $F_{\tilde{\gamma}_k}(\gamma)$, as

$$F_{\tilde{\gamma}_k}(\gamma) = 1 - \left(1 - \tilde{\Gamma}(m_0, \beta_0 \gamma)\right)\left(1 - \tilde{\Gamma}(m_k, \beta_k \gamma)\right). \tag{7}$$

Correspondingly, we derive the PDF of $\tilde{\gamma}_{k,b}$, $f_{\tilde{\gamma}_k}(\gamma)$, by taking the first derivative of (7) with respect to γ, which yields

$$f_{\tilde{\gamma}_k}(\gamma) = \frac{\beta_0^{m_0}}{\Gamma(m_0)} \gamma^{m_0 - 1} e^{-\beta_0 \gamma} \left(1 - \tilde{\Gamma}(m_k, \beta_k \gamma)\right) + \frac{\beta_k^{m_k}}{\Gamma(m_k)} \gamma^{m_k - 1} e^{-\beta_k \gamma} \left(1 - \tilde{\Gamma}(m_0, \beta_0 \gamma)\right). \tag{8}$$

[1] We highlight that the instantaneous SNRs for $\{D_k\}_{k=1}^K$ are non-identically distributed, due to the consideration of different distances $\{d_{R,D_k}\}_{k=1}^K$ and different channel gains $\{|h_{D_k,b}|^2\}_{k=1}^K$. We also highlight that the average SNRs for $\{D_k\}_{k=1}^K$ are different, due to the consideration of different distances $\{d_{R,D_k}\}_{k=1}^K$.}

B. Proposed Scheme

We detail the proposed partial CQI feedback scheme in this subsection. Prior to data transmission, the CQI values in the S–R and R–D_k links are measured using pilot sub-carriers transmitted by S and R, respectively, and fed back. We assume that the measurement and feedback of CQI are free of error. We denote $Z_{0,b}$ as the CQI in the S-R link on RB b, the value of which is calculated based on $\gamma_{0,b}$. We also denote $Z_{k,b}$ as the CQI in the R–D_k link on RB b the value of which is calculated based on $\gamma_{k,b}$. The calculation of $Z_{0,b}$ from $\gamma_{0,b}$ and the calculation of $Z_{k,b}$ from $\gamma_{k,b}$ will be later specified in Section III. Our proposed scheme is performed in two steps: 1) partial feedback and 2) opportunistic scheduling. These two steps are detailed as follows:

1) Partial Feedback: This step is completed in two consecutive phases. In the first phase, D_k compares its M_{RB} values of CQI and determines the highest M_{FB} values out of M_{RB} values. Then, D_k feeds back the M_{FB} CQI values along with their RB indices and the destination index k to R. In the second phase, if R receives CQI feedback for RB b from D_k, it calculates the equivalent end-to-end CQI of the S–R–D_k link, $\tilde{Z}_{k,b}$, which is given by

$$\tilde{Z}_{k,b} = \min\{Z_{0,b}, Z_{k,b}\}. \tag{9}$$

We clarify that the equivalent end-to-end CQIs are calculated based on the M_{FB} RBs for each destination, rather than the M_{RB} RBs. This is the benefit offered by the adoption of partial feedback. Notably, our partial feedback scheme considerably decreases the feedback overhead compared to the full feedback scheme where all the M_{RB} values are conveyed back from D_k to R [37]. Moreover, compared to the best-M feedback scheme [14], our two-phase feedback scheme enables S to obtain the equivalent end-to-end CQI of the S–R–D_k link. After determining $\tilde{Z}_{k,b}$ using (9), R feeds back $\tilde{Z}_{k,b}$, the RB index b, and the destination index k to S.

2) Opportunistic Scheduling: This step commences when S receives $\tilde{Z}_{k,b}$ along with the RB index b and the destination index k from R. Since D_k selects the M_{FB} out of M_{RB} CQI values independently, the number of CQI values on RB b, ν_b, received by S is lower than or equal to K, i.e. $\nu_b \leq K$. To facilitate the discussion, we define the set including the indices of the destinations which feed back CQI for RB b to R as $\mathcal{K}_b = \{k_b(q)\}_{q=1}^{\nu_b}$. Based on the received information, S estimates the equivalent end-to-end SNR on RB b for $D_{k_b(q)}$, $\tilde{\gamma}_{k_b(q),b}$. As per the principles of opportunistic scheduling, the scheduled destination for transmission on RB b, k_b^*, is determined via the criterion given by

$$k_b^* = \underset{q=1,2,\cdots,\nu_b}{\arg\max} \left\{\tilde{\gamma}_{k_b(q),b}\right\}. \tag{10}$$

After determining k_b^*, S assigns RB b to destination k_b^* and enables data transmission. When R forwards the regenerated data in the second phase, the data for destination k_b^* is also conveyed on RB b. This assignment guarantees that the data for different users is conveyed on different RBs. We note that there is a possibility in the scheme that no CQI on some RBs is fed back, i.e., $|\mathcal{K}_b| = 0$. In this case, no data is conveyed on these RBs. We clarify that $|\mathcal{K}_b| = 0$ does not contribute to the calculation of the sum rate. In the following section, we will conduct the sum rate analysis for the case of $|\mathcal{K}_b| \neq 0$.

III. Sum Rate Analysis

In this section, we derive new closed-form expressions for the sum rate of the MRN employing our proposed scheme in generalized Nakagami-m fading channels. Specifically, we consider two scenarios: 1) ideal CQI feedback and 2) quantized CQI feedback.

A. Ideal CQI Feedback

In this subsection, we consider the scenario of ideal CQI feedback where the accurate value of $\tilde{\gamma}_{k,b}$ is estimated from the feedback CQI. The performance analysis for this scenario allows us to quantify the maximum sum rate without considering the loss incurred by CQI quantization.

In MRNs, opportunistic scheduling is achieved by assigning the RB to the destination with the highest end-to-end instantaneous SNR out of K destinations, at any particular time. Therefore, for ideal CQI feedback, the effective CQI in the S-R link on RB b is given by

$$Z_{0,b}^{(\mathrm{I})} = \frac{\gamma_{0,b}}{\rho_{\mathrm{R}}}, \tag{11}$$

and the effective CQI in the R $-$ D_k link on RB b is given by

$$Z_{k,b}^{(\mathrm{I})} = \frac{\gamma_{k,b}}{\rho_{\mathrm{R}}}. \tag{12}$$

Based on (9), the end-to-end CQI for ideal CQI feedback is calculated by R using $\tilde{Z}_{k,b}^{(\mathrm{I})} = \min\{Z_{0,b}^{(\mathrm{I})}, Z_{k,b}^{(\mathrm{I})}\}$.

The exact sum rate of the MRN is obtained by averaging the transmission rates over all RBs $b = 1, 2, \cdots, M_{\mathrm{RB}}$. From (10), we define

$$X_{k_b^*}^{(\mathrm{I})} = \max_{q=1,2,\cdots,\nu_b} \left\{\tilde{Z}_{k_b(q),b}^{(\mathrm{I})} \rho_{\mathrm{R}}\right\}. \tag{13}$$

Then the exact sum rate can be derived by calculating the expectation of the rate with respect to the received SNR $\tilde{\gamma}_{k_b^*,b}$ on all the RBs, which can be expressed as

$$R_{\mathrm{sum}} = \mathbb{E}\left[\frac{1}{2}\log_2\left(1 + \tilde{\gamma}_{k_b^*,b}\right)\right], \tag{14}$$

where the factor $\frac{1}{2}$ is due to the fact that the transmission is over two consecutive time slots. From (13), we have $X_{k_b^*}^{(\mathrm{I})} = \tilde{\gamma}_{k_b^*,b}$. Moreover, $\{X_{k_b^*}^{(\mathrm{I})}\}_{b=1}^{M_{\mathrm{RB}}}$ have the equal likelihood of $\frac{1}{M_{\mathrm{RB}}}$ over all RBs. According to [38], the exact sum rate for ideal CQI feedback is derived as

$$\begin{aligned} R_{\mathrm{sum}}^{(\mathrm{I})} &= \sum_{b=1}^{M_{\mathrm{RB}}} \frac{1}{M_{\mathrm{RB}}} \mathbb{E}\left[\frac{1}{2}\log_2\left(1 + X_{k_b^*}^{(\mathrm{I})}\right)\right] \\ &\overset{(a)}{=} \frac{1}{2\log 2} \mathbb{E}\left[\log\left(1 + X_{k_b^*}^{(\mathrm{I})}\right)\right] \\ &= \frac{1}{2K\log 2} \sum_{k=1}^{K} \int_0^{\infty} \log(1+\gamma)\, d\left(F_{X_{k_b^*}^{(\mathrm{I})}}(\gamma)\right), \end{aligned} \tag{15}$$

where $F_{X^{(\mathrm{I})}_{k_b^*}}(\gamma)$ is the CDF of $X^{(\mathrm{I})}_{k_b^*}$. In (15), (a) follows from the fact that the instantaneous SNRs are independent and identically distributed with respect to RBs. In addition, $\frac{1}{2M_{\mathrm{RB}}}$ in (15) captures the two time slot transmission and the M_{RB} RBs in each time slot.

Observing (15), we find that the key to calculate $R^{(\mathrm{I})}_{\mathrm{sum}}$ is to derive $F_{X^{(\mathrm{I})}_{k_b^*}}(\gamma)$. As such, we express $F_{X^{(\mathrm{I})}_{k_b^*}}(\gamma)$ as

$$\begin{aligned} F_{X^{(\mathrm{I})}_{k_b^*}}(\gamma) &= \Pr\left(X^{(\mathrm{I})}_{k_b^*} < \gamma\right) \\ &\overset{(\mathrm{b})}{=} \sum_{\mathcal{K}_b} \Pr\left(\mathcal{K}_b\right) \Pr\left(X^{(\mathrm{I})}_{k_b^*} < \gamma | k \in \mathcal{K}_b\right) \\ &\overset{(\mathrm{c})}{=} \sum_{\mu=0}^{K} \Pr\left(|\mathcal{K}_b| = \mu\right) \Pr\left(X^{(\mathrm{I})}_{k_b^*} < \gamma \,\middle|\, |\mathcal{K}_b| = \mu\right), \end{aligned} \quad (16)$$

where (b) follows the total probability law and (c) is due to the fact that $\Pr\left(|\mathcal{K}_b| = \mu\right) \Pr\left(X^{(\mathrm{I})}_{k_b^*} < \gamma | |\mathcal{K}_b| = \mu\right)$ is only determined by μ, i.e. the size of $\mathcal{K}_b$, but not by the identity of the μ entities in $\mathcal{K}_b$. To derive $F_{X^{(\mathrm{I})}_{k_b^*}}(\gamma)$, we next derive $\Pr(|\mathcal{K}_b| = \mu)$ in *Step 1* and derive $\Pr\left(X^{(\mathrm{I})}_{k_b^*} < \gamma \,\middle|\, |\mathcal{K}_b| = \mu\right)$ in *Step 2*.

Step 1: Since each of the M_{RB} RBs is selected independently, the probability that M_{FB} RBs are selected to feed back CQI is $M_{\mathrm{FB}}/M_{\mathrm{RB}}$. Moreover, we find that $|\mathcal{K}_b|$ follows the binomial distribution with the probability mass function [39], which is due to the fact that the channel is independent among the destinations. As such, we derive $\Pr(|\mathcal{K}_b| = \mu)$ as

$$\begin{aligned} \Pr\left(|\mathcal{K}_b| = \mu\right) &\triangleq \Xi\left[\frac{M_{\mathrm{FB}}}{M_{\mathrm{RB}}}, K, \mu\right] \\ &= \binom{K}{\mu} \left(\frac{M_{\mathrm{FB}}}{M_{\mathrm{RB}}}\right)^{\mu} \left(1 - \frac{M_{\mathrm{FB}}}{M_{\mathrm{RB}}}\right)^{K-\mu}. \end{aligned} \quad (17)$$

Step 2: Since RB b is arranged to a single destination in the two consecutive time slots, $\tilde{Z}^{(\mathrm{I})}_{k_b(q),b}$ is independently distributed at RB b. Thus, applying (13) with the results of order statistics [36], we derive $\Pr\left(X^{(\mathrm{I})}_{k_b^*} < \gamma \,\middle|\, |\mathcal{K}_b| = \mu\right)$ as

$$\Pr\left(X^{(\mathrm{I})}_{k_b^*} < \gamma \,\middle|\, |\mathcal{K}_b| = \mu\right) = \left(F^{(\mathrm{I})}_{Y_{k,b}}(\gamma)\right)^{\mu}, \quad (18)$$

where $F_{Y^{(\mathrm{I})}_{k,b}}$ denotes the CDF of $Y^{(\mathrm{I})}_{k,b}$, and $Y^{(\mathrm{I})}_{k,b}$ denotes the SNR in the $\mathrm{S}-\mathrm{R}-\mathrm{D}_k$ link at the RBs that feed back CQI. With the aid of Lemma 1 in [15], we obtain $F_{Y^{(\mathrm{I})}_{k,b}}(\gamma)$ as

$$F_{Y^{(\mathrm{I})}_{k,b}}(\gamma) = \sum_{t=0}^{M_{\mathrm{FB}}-1} e_1\left[M_{\mathrm{RB}}, M_{\mathrm{FB}}, t\right] \left(F_{\tilde{\gamma}_k}(\gamma)\right)^{M_{\mathrm{RB}}-t}, \quad (19)$$

where

$$e_1\left[M_{\mathrm{RB}}, M_{\mathrm{FB}}, t\right] = \sum_{\tau=t}^{M_{\mathrm{FB}}-1} \frac{M_{\mathrm{FB}}-\tau}{M_{\mathrm{FB}}} \binom{M_{\mathrm{RB}}}{\tau} \binom{\tau}{t} (-1)^{\tau-t}.$$

Substituting (19) into (18), we obtain

$$\Pr\left(X^{(\mathrm{I})}_{k_b^*} < \gamma \,\middle|\, |\mathcal{K}_b| = \mu\right) = \sum_{\kappa=0}^{\mu(M_{\mathrm{FB}}-1)} \varepsilon_{\mu,\kappa} \left(F_{\tilde{\gamma}_k}(\gamma)\right)^{\mu M_{\mathrm{RB}}-\kappa}, \quad (20)$$

where $\varepsilon_{\mu,\kappa}$ is the $(\kappa+1)$-th entry of $\mathbf{e}_{\mu} = \underbrace{\mathbf{e}_1 * \mathbf{e}_1 * \cdots * \mathbf{e}_1}_{\mu}$ with $\mathbf{e}_1 = [e_1[M_{\mathrm{RB}}, M_{\mathrm{FB}}, 0] \cdots e_1[M_{\mathrm{RB}}, M_{\mathrm{FB}}, M_{\mathrm{FB}}-1]]$. Here, we denote $\mathbf{x} * \mathbf{y}$ as the convolution between $\mathbf{x}$ and $\mathbf{y}$ and denote $\underbrace{\mathbf{x} * \mathbf{x} * \cdots * \mathbf{x}}_{M}$ as the M times repeated convolution of $\mathbf{x}$. Aided by [15, Eq. (11)], we obtain $\varepsilon_{\mu,\kappa} = e_2[M_{\mathrm{RB}}, M_{\mathrm{FB}}, \mu, \kappa]$, where $e_2[M_{\mathrm{RB}}, M_{\mathrm{FB}}, \mu, \kappa]$ is given by (21), shown at the bottom of the page. Substituting (17) and (20) into (16), we derive $F_{X^{(\mathrm{I})}_{k_b^*}}(\gamma)$ as

$$\begin{aligned} F_{X^{(\mathrm{I})}_{k_b^*}}(\gamma) &= \sum_{\mu=0}^{K} \Xi\left[\frac{M_{\mathrm{FB}}}{M_{\mathrm{RB}}}, K, \mu\right] \\ &\quad \times \sum_{\kappa=0}^{\mu(M_{\mathrm{FB}}-1)} \varepsilon_{\mu,\kappa} \left(F_{\tilde{\gamma}_k}(\gamma)\right)^{\mu M_{\mathrm{RB}}-\kappa} \\ &= \Xi\left[\frac{M_{\mathrm{FB}}}{M_{\mathrm{RB}}}, K, 0\right] + \sum_{\mu=1}^{K} \Xi\left[\frac{M_{\mathrm{FB}}}{M_{\mathrm{RB}}}, K, \mu\right] \\ &\quad \times \sum_{\kappa=0}^{\mu(M_{\mathrm{FB}}-1)} \varepsilon_{\mu,\kappa} \left(F_{\tilde{\gamma}_k}(\gamma)\right)^{\mu M_{\mathrm{RB}}-\kappa}. \end{aligned} \quad (22)$$

Substituting (22) into (15), the exact sum rate for ideal CQI feedback is derived as

$$\begin{aligned} R^{(\mathrm{I})}_{\mathrm{sum}} = \frac{1}{2K} \sum_{k=1}^{K} \sum_{\mu=1}^{K} \Xi\left[\frac{M_{\mathrm{FB}}}{M_{\mathrm{RB}}}, K, \mu\right] \sum_{\kappa=0}^{\mu(M_{\mathrm{FB}}-1)} \varepsilon_{\mu,\kappa} \\ \times I_1(\mu M_{\mathrm{RB}} - \kappa; m_0, m_k, \beta_0, \beta_k), \end{aligned} \quad (23)$$

where $I_1(N; m_0, m_k, \beta_0, \beta_k)$ is given by

$$I_1(N; m_0, m_k, \beta_0, \beta_k) = \int_0^{\infty} \log_2(1+\gamma) d\left(F_{\tilde{\gamma}_k}(\gamma)\right)^N. \quad (24)$$

$$e_2[M_{\mathrm{RB}}, M_{\mathrm{FB}}, \mu, \kappa] = \begin{cases} (e_1[M_{\mathrm{RB}}, M_{\mathrm{FB}}, 0])^{\mu}, & \kappa = 0 \\ \sum_{\tau=1}^{\min\{\kappa, M_{\mathrm{FB}}-1\}} \frac{((\mu+1)\tau-\kappa) e_1[M_{\mathrm{RB}}, M_{\mathrm{FB}}, \tau] e_2[M_{\mathrm{RB}}, M_{\mathrm{FB}}, \mu, \kappa-\tau]}{\kappa e_1[M_{\mathrm{RB}}, M_{\mathrm{FB}}, 0]}, & 1 \le \kappa < \mu(M_{\mathrm{FB}}-1) \\ (e_1[M_{\mathrm{RB}}, M_{\mathrm{FB}}, M_{\mathrm{FB}}-1])^{\mu}, & \kappa = \mu(M_{\mathrm{FB}}-1) \end{cases} \quad (21)$$

When m_0 and m_k are integers, (24) is derived in closed-form as

$$\begin{aligned} &I_1(N; m_0, m_k, \beta_0, \beta_k) \\ &= \frac{N}{(\hat{m}_k-1)!\log 2}\sum_{n=0}^{N-1}\binom{N-1}{n}(-1)^n e^{(n+1)(\beta_0+\beta_k)} \\ &\quad\times \sum_{\ell=0}^{\tilde{m}_{k,n}} w_{k,n,\ell}(\hat{m}_k+\ell-1)! \\ &\quad\times \sum_{j=1}^{\hat{m}_k+\ell}\frac{\hat{\Gamma}(j-\hat{m}_k-\ell,(n+1)(\beta_0+\beta_k))}{[(n+1)(\beta_0+\beta_k)]^j}, \end{aligned} \tag{25}$$

where $\tilde{m}_{k,n}=n(m_0+m_k-2)+\check{m}_k-1$, $\hat{m}_k=\min\{m_0,m_k\}$, $\check{m}_k=\max\{m_0,m_k\}$, and $\hat{\Gamma}(\alpha,x)$ denotes the incomplete gamma function [33, Eq. (8.350.1)] given by $\hat{\Gamma}(\alpha,x)=\int_0^x e^{-t}t^{\alpha-1}dt$. When $\alpha=-q$, $q\in\mathbb{N}^+$, $\hat{\Gamma}(-q,x)$ is calculated as $\hat{\Gamma}(-q,x)=\frac{(-1)^q}{q!}\left[E_1(x)-e^{-x}\sum_{\rho=0}^{q-1}\frac{(-1)^\rho\rho!}{x^{\rho+1}}\right]$, where $E_1(x)$ is the exponential integral function of the first kind [40, Eq. (5.1.1)] given by $E_1(x)=\int_x^\infty\frac{e^{-t}}{t}dt$. The variable $w_{k,n,\ell}$ is the $(\ell+1)$-th entry of $\mathbf{w}_{k,n}$, where

$$\mathbf{w}_{k,n}=\mathbf{a}_k*\underbrace{\mathbf{c}_0*\cdots*\mathbf{c}_0}_{n}*\underbrace{\mathbf{c}_k*\cdots*\mathbf{c}_k}_{n}. \tag{26}$$

In (26), we define $\mathbf{a}_k=[a_0\ \ a_1\ \ \cdots\ \ a_{\check{m}_k-1}]$, where if $m_0=m_k$, a_ϵ is given by

$$a_\epsilon=\frac{\beta_k^{m_k}\beta_0^\epsilon+\beta_0^{m_0}\beta_k^\epsilon}{\epsilon!}, \tag{27}$$

if $m_0<m_k$, a_ϵ is given by

$$a_\epsilon=\begin{cases}\frac{\beta_k^{m_k}\beta_0^\epsilon\Gamma(m_0)}{\epsilon!\Gamma(m_k)}, & 0\le\epsilon\le m_k-m_0-1\\ \frac{\beta_k^{m_k}\beta_0^\epsilon\Gamma(m_0)}{\epsilon!\Gamma(m_k)}+\frac{\beta_0^{m_0}\beta_k^\epsilon}{\epsilon!}, & m_k-m_0\le\epsilon\le m_k-1,\end{cases} \tag{28}$$

and if $m_0>m_k$, a_ϵ is given by

$$a_\epsilon=\begin{cases}\frac{\beta_0^{m_0}\beta_k^\epsilon\Gamma(m_k)}{\epsilon!\Gamma(m_0)}, & 0\le\epsilon\le m_0-m_k-1\\ \frac{\beta_0^{m_0}\beta_k^\epsilon\Gamma(m_k)}{\epsilon!\Gamma(m_0)}+\frac{\beta_k^{m_k}\beta_0^\epsilon}{\epsilon!}, & m_0-m_k\le\epsilon\le m_0-1.\end{cases} \tag{29}$$

In (26), we further define $\mathbf{c}_0=\left[1\beta_0\frac{\beta_0^2}{2!}\cdots\frac{\beta_0^{m_0-1}}{(m_0-1)!}\right]$ and $\mathbf{c}_k=\left[1\beta_k\frac{\beta_k^2}{2!}\cdots\frac{\beta_k^{m_k-1}}{(m_k-1)!}\right]$. The detailed proof of (25) is given in Appendix A. Finally, the exact sum rate for ideal CQI feedback is derived in (30), shown at the bottom of the page, where $\lambda_{k,n}=(n+1)(\beta_0+\beta_k)$.

Based on (30), we present simplified results for some special cases, as follows.

Case 1: MRN subject to i.i.d. Rayleigh fading with $m_0=m_1=\cdots=m_k=1$. In this case, (30) is simplified as

$$\begin{aligned} R_{\text{sum}}^{(\text{I})} &= \frac{1}{2K\log 2}\sum_{k=1}^{K}\sum_{\mu=1}^{K}\Xi\left[\frac{M_{\text{FB}}}{M_{\text{RB}}},K,\mu\right] \\ &\quad\times\sum_{\kappa=0}^{\mu(M_{\text{FB}}-1)}\varepsilon_{\mu,\kappa}(\mu M_{\text{RB}}-\kappa)\sum_{n=0}^{\mu M_{\text{RB}}-\kappa-1}(-1)^n \\ &\quad\times w_{k,n,0}\binom{\mu M_{\text{RB}}-\kappa-1}{n}\frac{e^{\lambda_{k,n}}}{\lambda_{k,n}}E_1(\lambda_{k,n}). \end{aligned} \tag{31}$$

we note that (31) can be derived based on [15, Eq. (13)] which is the throughput of multiuser networks over Rayleigh fading.

Case 2: Single-user relay network with $K=1$. In this case, (30) is simplified as

$$\begin{aligned} R_{\text{sum}}^{(\text{I})} &= \frac{M_{\text{FB}}}{2(\hat{m}_1-1)!M_{\text{RB}}\log 2}\sum_{\kappa=0}^{M_{\text{FB}}-1}\varepsilon_{1,\kappa}\sum_{n=0}^{M_{\text{RB}}-\kappa-1}e^{\lambda_{n,1}} \\ &\quad\times\binom{M_{\text{RB}}-\kappa-1}{n}\sum_{\ell=0}^{\tilde{m}_{1,n}}(-1)^n w_{1,n,\ell} \\ &\quad\times(\hat{m}_1+\ell-1)!\sum_{j=1}^{\hat{m}_1+\ell}\frac{(-1)^{\hat{m}_1+\ell-j}}{\lambda_{1,n}^j(\hat{m}_1+\ell-j)!} \\ &\quad\times\left(E_1(\lambda_{1,n})-e^{-\lambda_{1,n}}\sum_{\rho=0}^{\hat{m}_1+\ell-j-1}\frac{(-1)^\rho\rho!}{\lambda_{k,n}^{\rho+1}}\right). \end{aligned} \tag{32}$$

We note that multiuser diversity gain vanishes when $K=1$. As such, (32) is equivalent to the average rate of a point-to-point relay-aided system in Nakagami-m fading channels, where optimal rate control [41] is applied among the best M_{FB} out of M_{RB} RBs.

Case 3: Each destination feeds back the CQI of only the best RB to the source. In this case, (30) is simplified as

$$\begin{aligned} R_{\text{sum}}^{(\text{I})} &= \sum_{k=1}^{K}\frac{M_{\text{RB}}}{2K(\hat{m}_k-1)!\log 2}\sum_{\mu=1}^{K}\Xi\left[\frac{1}{M_{\text{RB}}},K,\mu\right]\varepsilon_{\mu,0} \\ &\quad\times\mu\sum_{n=0}^{\mu M_{\text{RB}}-1}(-1)^n\sum_{\ell=0}^{\tilde{m}_{k,n}}w_{k,n,\ell}\binom{\mu M_{\text{RB}}-1}{n} \\ &\quad\times(\hat{m}_k+\ell-1)!e^{\lambda_{k,n}}\sum_{j=1}^{\hat{m}_k+\ell}\frac{(-1)^{\hat{m}_k+\ell-j}}{\lambda_{k,n}^j(\hat{m}_k+\ell-j)!} \\ &\quad\times\left(E_1(\lambda_{k,n})-e^{-\lambda_{k,n}}\sum_{\rho=0}^{\hat{m}_k+\ell-j-1}\frac{(-1)^\rho\rho!}{\lambda_{k,n}^{\rho+1}}\right). \end{aligned} \tag{33}$$

$$\begin{aligned} R_{\text{sum}}^{(\text{I})} &= \sum_{k=1}^{K}\frac{1}{2K(\hat{m}_k-1)!\log 2}\sum_{\mu=1}^{K}\Xi\left[\frac{M_{\text{FB}}}{M_{\text{RB}}},K,\mu\right]\sum_{\kappa=0}^{\mu(M_{\text{FB}}-1)}\varepsilon_{\mu,\kappa}\sum_{n=0}^{\mu M_{\text{RB}}-\kappa-1}\sum_{\ell=0}^{\tilde{m}_{k,n}}(\mu M_{\text{RB}}-\kappa)\binom{\mu M_{\text{RB}}-\kappa-1}{n} \\ &\quad\times(-1)^n w_{k,n,\ell}(\hat{m}_k+\ell-1)!e^{\lambda_{k,n}}\sum_{j=1}^{\hat{m}_k+\ell}\frac{(-1)^{\hat{m}_k+\ell-j}}{\lambda_{k,n}^j(\hat{m}_k+\ell-j)!}\times\left(E_1(\lambda_{k,n})-e^{-\lambda_{k,n}}\sum_{\rho=0}^{\hat{m}_k+\ell-j-1}\frac{(-1)^\rho\rho!}{\lambda_{k,n}^{\rho+1}}\right) \end{aligned} \tag{30}$$

We highlight that (33) can be viewed as an extension of [42, Eq. (11)] to the MRN in Nakagami-m fading.

Case 4: Full feedback with $M_{\rm FB} = M_{\rm RB}$. In this case, aided with [15, Corollary 1], (30) is simplified as

$$R_{\rm sum}^{(\rm I)} = \sum_{k=1}^{K} \frac{1}{2(\hat{m}_k - 1)! \log 2} \sum_{n=0}^{K-1} (-1)^n \times \sum_{\ell=0}^{\tilde{m}_{k,n}} w_{k,n,\ell} (\hat{m}_k + \ell - 1)! \binom{K-1}{n} e^{\lambda_{k,n}} \times \sum_{j=1}^{\hat{m}_k+\ell} \frac{(-1)^{\hat{m}_k+\ell-j}}{\lambda_{k,n}^{j} (\hat{m}_k + \ell - j)!} \times \left(E_1(\lambda_{k,n}) - e^{-\lambda_{k,n}} \sum_{\rho=0}^{\hat{m}_k+\ell-j-1} \frac{(-1)^{\rho} \rho!}{\lambda_{k,n}^{\rho+1}} \right). \quad (34)$$

Note that in the presence of full feedback, the sum rate is not affected by $M_{\rm RB}$. It is equivalent to the sum rate of the MRN with a single carrier in the downlink [34].

B. Quantized CQI Feedback

In this subsection, we consider the scenario of quantized CQI feedback where the indices of the quantized CQI regions are fed back from the receiver to the transmitter. We highlight that quantized CQI further reduces the feedback overhead relative to ideal CQI which mandates the exact CQI values in the feedback channel. The performance analysis for this scenario allows us to examine the impact of quantization parameters on the sum rate.

For quantized CQI feedback, the CQI of the R $-$ D$_k$ link on RB b is defined as

$$Z_{k,b}^{(\rm Q)} = Q\left(Z_{k,b}^{(\rm I)}\right) \quad (35)$$

with

$$Q\left(Z_{k,b}^{(\rm I)}\right) = J_l, \text{ for } \xi_l \le Z_{k,b}^{(\rm I)} < \xi_{l+1} \text{ and } 1 \le l \le L, \quad (36)$$

where J_l denotes the index of quantization region, ξ_l denotes the boundary value between two quantization regions, $\xi_{L+1} = \infty$, and L denotes the number of quantization levels. We clarify that the indices of the quantized regions are fed back from D$_k$ to R. Similarly, the CQI in the S-R link on RB b is defined as

$$Z_{0,b}^{(\rm Q)} = Q\left(Z_{0,b}^{(\rm I)}\right). \quad (37)$$

As such, R calculates the quantized end-to-end CQI on RB b as $\tilde{Z}_{k,b}^{(\rm Q)} = \min\{Z_{0,b}^{(\rm Q)}, Z_{k,b}^{(\rm Q)}\}$.

For quantized CQI feedback, we define

$$X_{k_b^*}^{(\rm Q)} = \max_{q=1,2,\cdots,\nu_b} \left\{ \Theta\left(\tilde{Z}_{k_b(q),b}^{(\rm Q)}\right) \rho_{\rm R} \right\}, \quad (38)$$

where $\Theta(J_l) = \xi_l$. Accordingly, the exact sum rate for quantized CQI feedback is expressed as

$$R_{\rm sum}^{(\rm Q)} = \mathbb{E}_{|\mathcal{K}_b|} \mathbb{E}_{X_{k_b^*}^{(\rm Q)}} \left[\log_2(1 + X_{k_b^*}^{(\rm Q)}) \middle| |\mathcal{K}_b| \ne 0 \right] = \frac{1}{2K} \sum_{k=1}^{K} \sum_{l=1}^{L} \log_2(1 + \xi_l \rho_{\rm R}) \Pr(J_l || \mathcal{K}_b| = \mu). \quad (39)$$

In (39), we express $\Pr(J_l||\mathcal{K}_b| = \mu)$ as

$$\Pr(J_l||\mathcal{K}_b| = \mu) = \Pr(|\mathcal{K}_b| = \mu) \times \Pr\left(X_{k_b^*}^{(\rm Q)} = \xi_l \rho_{\rm R} || \mathcal{K}_b| = \mu\right). \quad (40)$$

We next use the results of order statistics [36] to derive $\Pr(X_{k_b^*}^{(\rm Q)} = \xi_l \rho_{\rm R}||\mathcal{K}_b| = \mu)$ in (40) as

$$\begin{aligned} &\Pr\left(X_{k_b^*}^{(\rm Q)} = \xi_l \rho_{\rm R} || \mathcal{K}_b| = \mu\right) \\ &= \Pr\left(\max_{k \in \mathcal{K}_b} Y_{k,b}^{(\rm Q)} \le \xi_{l+1}\right) - \Pr\left(\max_{k \in \mathcal{K}_b} Y_{k,b}^{(\rm Q)} \le \xi_l\right) \\ &= \left[\Pr\left(Y_{k,b}^{(\rm Q)} \le \xi_{l+1}\right)\right]^{\mu} - \left[\Pr\left(Y_{k,b}^{(\rm Q)} \le \xi_l\right)\right]^{\mu}. \end{aligned} \quad (41)$$

We note that the CDF of $Y_{k,b}^{(\rm Q)}$, $F_{Y_{k,b}^{(\rm Q)}}(\gamma)$, is equivalent to $F_{Y_{k,b}^{(\rm I)}}(\gamma)$ given by (19), the proof of which is given in Appendix B. As such, substituting (17), (40), and (41) into (39), we derive the closed-form expression for $R_{\rm sum}^{(\rm Q)}$ as

$$\begin{aligned} R_{\rm sum}^{(\rm Q)} &= \frac{1}{2K} \sum_{k=1}^{K} \sum_{\mu=1}^{K} \Xi\left[\frac{M_{\rm FB}}{M_{\rm RB}}, K, \mu\right] \sum_{l=1}^{L} \log_2(1 + \xi_l \rho_{\rm R}) \times \left[\left(F_{Y_{k,b}^{(\rm Q)}}(\xi_{l+1}\rho_{\rm R}) \right)^{\mu} - \left(F_{Y_{k,b}^{(\rm Q)}}(\xi_l \rho_{\rm R}) \right)^{\mu} \right] \\ &= \frac{1}{2K} \sum_{k=1}^{K} \sum_{\mu=1}^{K} \Xi\left[\frac{M_{\rm FB}}{M_{\rm RB}}, K, \mu\right] I_2(\mu; \xi_1, \cdots, \xi_L), \end{aligned} \quad (42)$$

where

$$I_2(\mu; \xi_1, \cdots, \xi_L) = \sum_{l=1}^{L} \log_2(1 + \xi_l \rho_{\rm R}) \times \left[\left(F_{Y_{k,b}^{(\rm Q)}}(\xi_{l+1}\rho_{\rm R}) \right)^{\mu} - \left(F_{Y_{k,b}^{(\rm Q)}}(\xi_l \rho_{\rm R}) \right)^{\mu} \right]..$$

Compared (42) with (23), the finite integral in (23) is replaced by the sum of the expectations of $\log_2(1 + \xi_l \rho_{\rm R})$ in the L quantization regions (42). As such, the exact sum rate in (42) can be viewed as the approximation of the exact sum rate for ideal CQI feedback. Importantly, the gap between (42) and (23) can be bridged as L increases, which will be shown in Section IV.

C. Asymptotic Sum Rate

In this section, we derive the asymptotic sum rates for ideal CQI, as $K \to \infty$. Here, the consideration of $K \to \infty$ corresponds to the scenario where a high density deployment of users are served in the network. The newly derived asymptotic result simplifies the exact expression for the exact sum rate in (23). We highlight that the asymptotic result for ideal CQI feedback can be used to approximate the sum rate for quantized CQI feedback with a large L.

In deriving $\hat{R}_{\rm sum}^{(\rm I)}$, we first find from Fig. 2 that for fixed m_0, m_1, β_0, and β_k, $I_1(N; m_0, m_k, \beta_0, \beta_k)$ is saturated when N grows large. We then find that $\Delta I_1(N; m_0, m_k, \beta_0, \beta_k)$ approaches zero for a large N. Therefore, we conclude that $I_1(\mu M_{\rm RB} - \kappa; m_0, m_k, \beta_0, \beta_k) \approx I_1(K; m_0, m_k, \beta_0, \beta_k)$ when $K \to \infty$. Furthermore, we find from (20) that $\sum_{\kappa=0}^{\mu(M_{\rm FB}-1)} \varepsilon_{\mu,\kappa} = 1$.

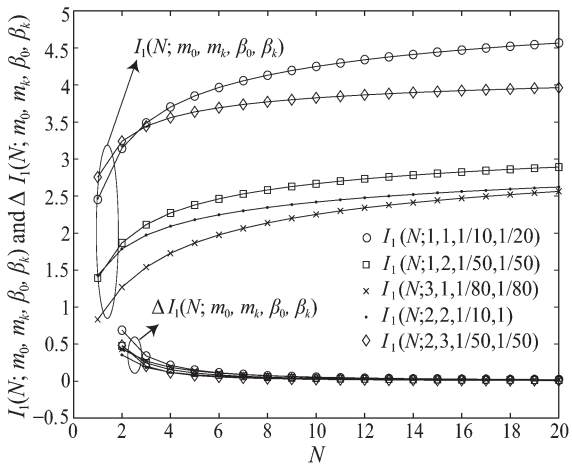

Fig. 2. $I_1(N; m_0, m_k, \beta_0, \beta_k)$ and $\Delta I_1(N; m_0, m_k, \beta_0, \beta_k) = I_1(N; m_0, m_k, \beta_0, \beta_k) - I_1(N-1; m_0, m_k, \beta_0, \beta_k)$ versus N for different values of m_0, m_k, β_0, and β_k.

As such, the asymptotic sum rate for ideal CQI feedback is derived as

$$\hat{R}_{\text{sum}}^{(\text{I})} = \sum_{k=1}^{K} \frac{I_1(K; m_0, m_k, \beta_0, \beta_k)}{2K} \sum_{\mu=1}^{K} \Xi\left[\frac{M_{\text{FB}}}{M_{\text{RB}}}, K, \mu\right] = \sum_{k=1}^{K} \frac{I_1(K; m_0, m_k, \beta_0, \beta_k)}{2K} \left[1 - \left(1 - \frac{M_{\text{FB}}}{M_{\text{RB}}}\right)^K\right]. \quad (43)$$

We clarify that the term $\left(1 - \frac{M_{\text{FB}}}{M_{\text{RB}}}\right)^K$ in (43) is the scheduling outage probability [13] (or equivalently, the feedback hole probability [14]), which characterizes the probability of that no CQI is fed back for a RB. It is easy to see that the scheduling outage probability decreases when $\frac{M_{FB}}{M_{RB}}$ increases, and approaches 0 as K grows large.

Based on (43), we offer four valuable insights as

1) The sum rate of our partial feedback scheme increases with K. This is due to the fact that $\hat{R}_{sum}^{(\text{I})}$ is a monotonically increasing function of K.
2) The sum rate of our partial feedback scheme becomes saturated in the large regime of K. This is due to the fact that in the large regime of K, $I_1(K; m_0, m_k, \beta_0, \beta_k)$ becomes saturated and the scheduling outage probability approaches zero.
3) The sum rate of our partial feedback scheme increases with M_{FB}. Notably, the sum rate of our partial feedback scheme approaches that of the full feedback scheme when M_{FB} approaches M_{RB}. This is due to the fact that the scheduling outage probability decreases and approaches 0 when M_{FB} increases and becomes close to M_{RB}.
4) The sum rate of our partial feedback scheme approaches that of the full feedback scheme for fixed M_{FB} and M_{RB}, when K grows large. This is due to the fact that the scheduling outage probability approaches 0 as $K \to \infty$.

These insights will be verified in Section IV.

We next present the asymptotic sum rate for some special cases. First, by setting $m_0 = m_1 =, \cdots, = m_K = 1$ in (43), the asymptotic result for *Case 1* is derived as

$$\hat{R}_{\text{sum}}^{(\text{I})} = \sum_{k=1}^{K} \frac{I_1(K; 1, 1, \beta_0, \beta_k)}{2K} \left[1 - \left(1 - \frac{M_{\text{FB}}}{M_{\text{RB}}}\right)^K\right]. \quad (44)$$

We highlight that (44) can be obtained with the aid of [15, Eq. (38)] which presents the asymptotic result for multiuser networks.

Second, we find that the asymptotic result for the single-user relay network in *Case 2* is not available since the asymptotic sum rate evaluates the performance as $K \to \infty$.

Third, the asymptotic result for 1-best feedback in *Case 3* is obtained as

$$\hat{R}_{\text{sum}}^{(\text{I})} = \sum_{k=1}^{K} \frac{I_1(K; m_0, m_k, \beta_0, \beta_k)}{2K} \left[1 - \left(1 - \frac{1}{M_{\text{RB}}}\right)^K\right]. \quad (45)$$

Comparing (45) with (43), we find that the gap between 1-best feedback and partial feedback decreases as K increases, which is due to the fact that $\left[1 - \left(1 - \frac{1}{M_{\text{RB}}}\right)^K\right] \to 0$ as $K \to \infty$.

Fourth, setting $M_{\text{FB}} = M_{\text{RB}}$ in (43), we obtain the asymptotic result for full feedback in *Case 4* as

$$\hat{R}_{\text{sum}}^{(\text{I})} = \sum_{k=1}^{K} \frac{I_1(K; m_0, m_k, \beta_0, \beta_k)}{2K}. \quad (46)$$

It is indicated from (46) that the asymptotic sum rate for full feedback does not depend on M_{RB}. It only depends on the number of users and the value of fading parameters. For the case of full feedback, the number of CQ values received by S for each RB is always K, which implies that scheduling outage does not occur. As such, M_{RB} has no impact on the asymptotic sum rate in such a case. By comparing (43) with (46), we conclude that the sum rate of partial feedback is an increasing function of a factor $[1 - (1 - \frac{M_{FB}}{M_{RB}})^K]$. This factor can be viewed as the sum rate loss caused by partial feedback.

IV. Numerical Results and Simulations

In this section, we present numerical results to examine the sum rate of the MRN for various channel parameters and network configurations. Throughout this section, we assume that the distances $d_{\text{S,R}}$ and $\{d_{\text{R,D}_k}\}_{k=1}^K$ are uniformly distributed among (0, 1], η is set to $\eta = 4$, and $m_0 = m_k = m$, $k \in \{1, \cdots, K\}$. The variance of the fading coefficients is normalized to unity with $\mathbb{E}[|h_{0,b}|^2] = \mathbb{E}[|h_{k,b}|^2] = 1$. In Figs. 3–9, we use solid lines to represent the exact sum rate for ideal CQI feedback, obtained from (30), dotted lines to represent the exact sum rate for quantized CQI feedback, obtained from (42), and dashed lines to represent the asymptotic sum rate for ideal CQI feedback, obtained from (43). We also use marks, e.g., '$\circ$', '$\triangle$', '$\diamond$', and '$+$', to represent Monte Carlo simulation points. The rate loss due to cyclic prefix is not included in the simulation, and will be considered in future work. In all

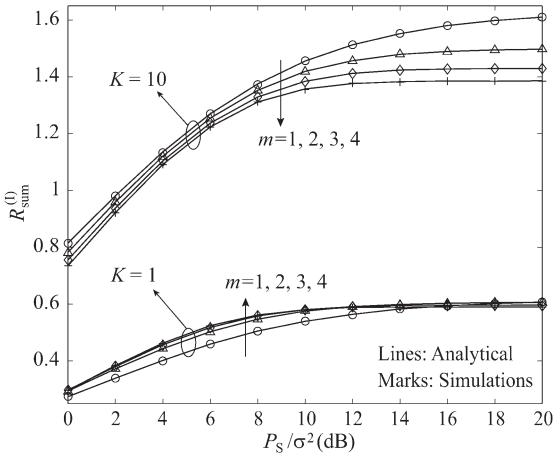

Fig. 3. $R_{\text{sum}}^{(\text{I})}$ versus P_{S}/σ^2 for $P_{\text{R}}/\sigma^2 = 5$ dB, $M_{\text{RB}} = 10$, $M_{\text{FB}} = 5$, and $d_{\text{S,R}} = d_{\text{R,D}_k} = 1, k \in \{1, \cdots, K\}$.

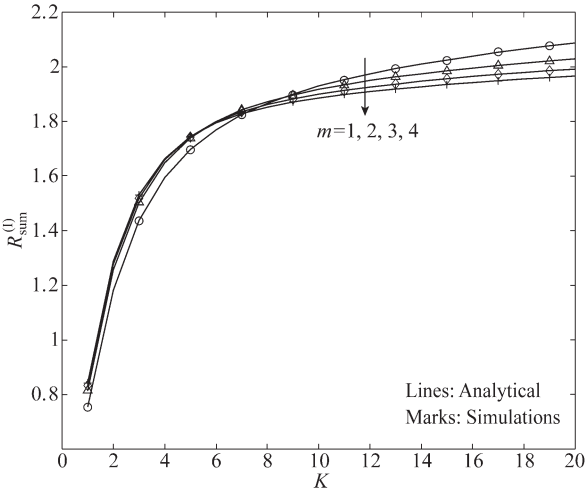

Fig. 4. $R_{\text{sum}}^{(\text{I})}$ versus K for $P_{\text{S}}/\sigma^2 = P_{\text{R}}/\sigma^2 = 10$ dB, $M_{\text{RB}} = 10$, $M_{\text{FB}} = 5$, and $d_{\text{S,R}} = d_{\text{R,D}_k} = 1, k \in \{1, \cdots, K\}$.

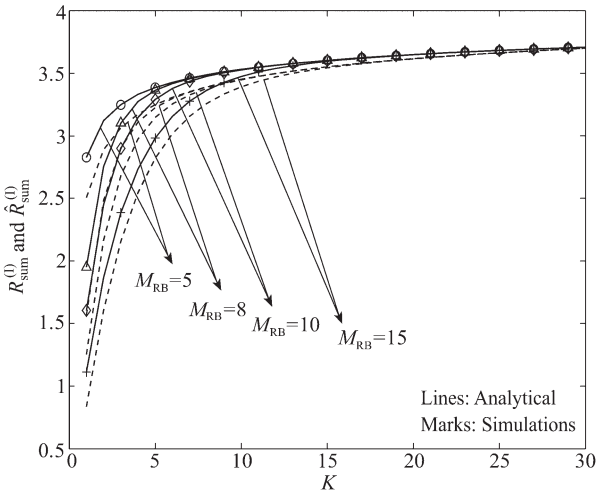

Fig. 5. $R_{\text{sum}}^{(\text{I})}$ and $\hat{R}_{\text{sum}}^{(\text{I})}$ versus K for $P_{\text{S}}/\sigma^2 = P_{\text{R}}/\sigma^2 = 20$ dB, $M_{\text{FB}} = 5$, $m = 2$, and $d_{\text{S,R}} = d_{\text{R,D}_k} = 1, k \in \{1, \cdots, K\}$.

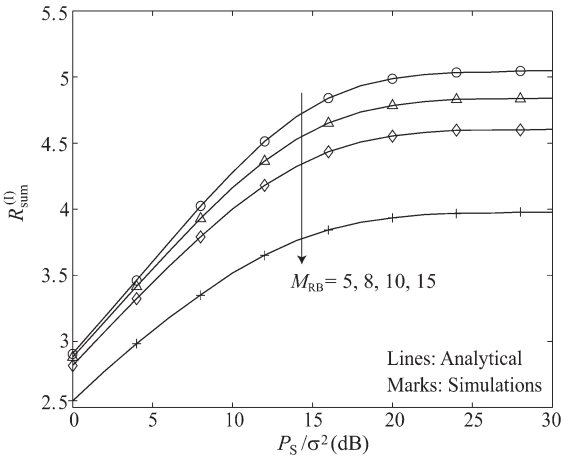

Fig. 6. $R_{\text{sum}}^{(\text{I})}$ versus P_{S}/σ^2 for $P_{\text{R}}/\sigma^2 = 5$ dB, $M_{\text{FB}} = 5$, and $K = 5$, where $d_{\text{S,R}}$ and $\{d_{\text{S,D}_k}\}_{k=1}^{K}$ are uniformly distributed among (0,1), and m_0 and $\{m_k\}_{k=1}^{K}$ are uniformly selected from set {1,2,3,4}.

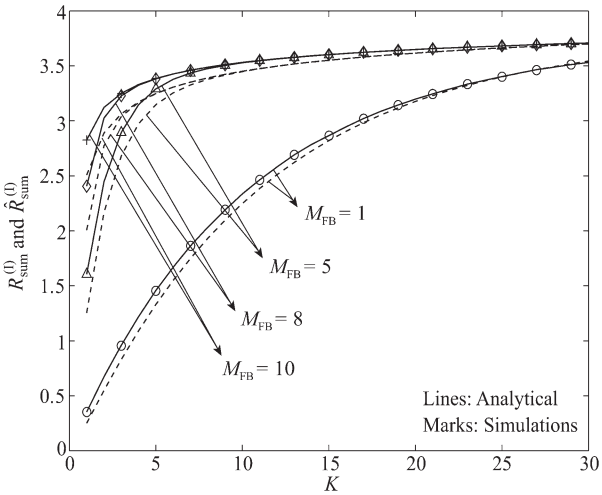

Fig. 7. $R_{\text{sum}}^{(\text{I})}$ and $\hat{R}_{\text{sum}}^{(\text{I})}$ versus P_{S}/σ^2 for $P_{\text{R}}/\sigma^2 = 20$ dB, $M_{\text{RB}} = 10$, $K = 10$, $m = 2$, and $d_{\text{S,R}} = d_{\text{R,D}_k} = 1, k \in \{1, \cdots, K\}$.

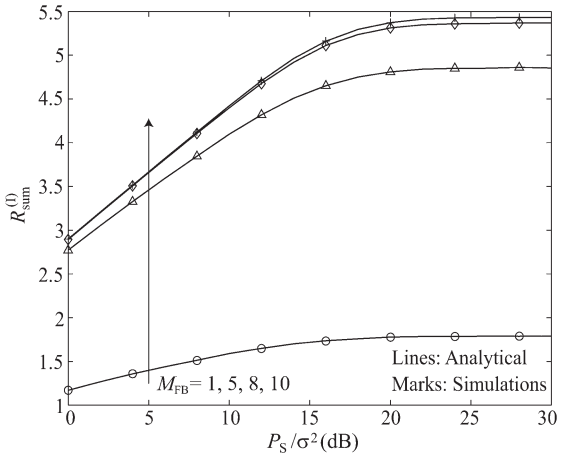

Fig. 8. $R_{\text{sum}}^{(\text{I})}$ versus P_{S}/σ^2 for $P_{\text{R}}/\sigma^2 = 5$ dB, $M_{\text{RB}} = 10$, and $K = 5$, where $d_{\text{S,R}}$ and $\{d_{\text{S,D}_k}\}_{k=1}^{K}$ are uniformly distributed among (0,1), and m_0 and $\{m_k\}_{k=1}^{K}$ are uniformly selected from set {1,2,3,4}.

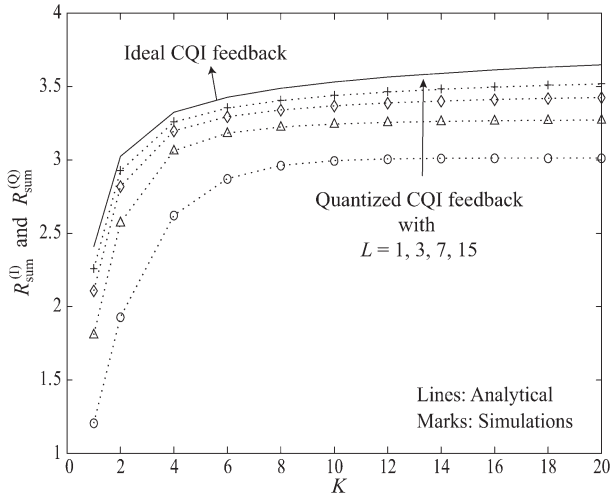

Fig. 9. $R_{\text{sum}}^{(\text{I})}$, $R_{\text{sum}}^{(\text{Q})}$, and $\hat{R}_{\text{sum}}^{(\text{Q})}$ versus K for $P_{\text{S}}/\sigma^2 = P_{\text{R}}/\sigma^2 = 20$ dB, $M_{\text{RB}} = 10$, $M_{\text{FB}} = 8$, $m = 2$, and $d_{\text{S,R}} = d_{\text{R,D}_k} = 1$, $k \in \{1, \cdots, K\}$.

the figures, we see a precise agreement between the simulation points and the analytical curves, which verifies the correctness of our theoretical expressions derived in Section III.

A. Impact of Nakagami-m Fading Parameter

In this subsection, we examine the effect of Nakagami-m fading parameter on the sum rate. Fig. 3 depicts the exact sum rate for ideal CQI feedback versus P_{S}/σ^2 for different Nakagami-m fading parameters and different number of users. We observe that when $K = 10$, increasing m yields a lower sum rate, while when $K = 1$, increasing m yields a slightly higher sum rate. This is due to the fact that the fading environment becomes more scattering and the fluctuations of the signal strength increase as m decreases [30], [31]. Such a more smattering fading environment is beneficial for multiuser scheduling, since the larger channel variation enables the scheduler to arrange transmissions at higher peaks of channel fading, especially when the number of users is high. As such, for $K = 10$ where multiuser diversity is efficiently exploited, the scheduler is able to arrange the transmission to the link with best channel quality. This leads to the fact that higher fluctuations of the received signal improves the sum rate. On the other hand, for $K = 1$ where no multiuser diversity is exploited, the source transmits the downlink data to D_1 on M_{FB} RBs. It follows that higher fluctuations of the received signal reduces the sum rate.

Fig. 4 depicts the exact sum rate for ideal CQI feedback versus K for different fading parameters. We observe that a lower m is beneficial for the sum rate when K is large, e.g., $K \geq 8$, but detrimental for the sum rate when K is small, e.g., $K < 8$. We note that a more scattering environment caused by a lower m is theoretically beneficial for the multiuser diversity [34]. However, this figure shows that this benefit can only be reaped in the large K regime, due to the partial feedback of CQI.

B. Impact of M_{RB} and M_{FB}

In this subsection, we first examine the impact of M_{RB} on the sum rate. Fig. 5 depicts the exact sum rate and the asymptotic sum rate for ideal CQI feedback versus K for different M_{RB}s. We first observe that the asymptotic curves accurately approximate the exact curves when K becomes large, which demonstrates the validity of our asymptotic result. We then observe that increasing M_{RB} brings a profound decrease in $R_{\text{sum}}^{(\text{I})}$ in the small K regime. In the large K regime, alternatively, the decrease in $R_{\text{sum}}^{(\text{I})}$ brought by increasing M_{RB} is almost negligible. To explain these observations, we denote $R_{\text{sum}}^{\text{ratio}}$ as the ratio between $R_{\text{sum}}^{(\text{I})}$ for partial feedback with $M_{\text{FB}} < M_{\text{RB}}$ and $R_{\text{sum}}^{(\text{I})}$ for full feedback with $M_{\text{FB}} = M_{\text{RB}}$, given by

$$R_{\text{sum}}^{\text{ratio}} = \frac{R_{\text{sum}}^{(\text{I})} \text{ for } M_{\text{FB}} < M_{\text{RB}}}{R_{\text{sum}}^{(\text{I})} \text{ for } M_{\text{FB}} = M_{\text{RB}}} \simeq 1 - \left(1 - \frac{M_{\text{FB}}}{M_{\text{RB}}}\right)^K. \quad (47)$$

Based on (47), we find that the value of $R_{\text{sum}}^{\text{ratio}}$ is determined by three terms, namely M_{FB}, M_{RB}, and K. When M_{FB} is fixed and K is small, increasing M_{RB} significantly decreases $R_{\text{sum}}^{\text{ratio}}$ and therefore decreases the sum rate. When K is large, M_{RB} has less impact on $R_{\text{sum}}^{\text{ratio}}$. This results in sum rates for different M_{RB}s approaching each other for a large K.

Fig. 6 depicts the exact sum rate for ideal CQI feedback versus P_{S}/σ^2 for different M_{RB}s. We observe that the sum rate significantly increases in the low SNR regime, but is saturated in the high SNR regime. This is due to the fact that the sum rate of MRN is limited by the weaker hop. In addition, we observe that the rate gap among the curves almost keeps as a constant in the high SNR regime. As such, the rate gap between the M_{RB}s cannot be compensated by simply increasing the SNR. Based on Figs. 5 and 6, we conclude that when the feedback overhead is fixed, the performance of MRN is improved by reducing the number of RBs.

We next examine the impact of M_{FB} on the sum rate. Fig. 7 depicts the exact sum rate and the asymptotic sum rate for ideal CQI feedback versus K for different M_{FB}s. We first observe that full CQI feedback with $M_{\text{FB}} = M_{\text{RB}} = 10$ outperforms partial CQI feedback with $M_{\text{FB}} < M_{\text{RB}}$. This performance advantage is pronounced in the small K regime, but negligible in the large K regime. These observations result from the fact that $R_{\text{sum}}^{\text{ratio}}$ in (47) increases significantly with M_{FB} when M_{RB} is fixed and K is small. When K is large, the impact of M_{FB} is less predominant. This in turn results in a decrease in the rate gap in the large K regime. Note that the performance of 1-CQI feedback with $M_{\text{FB}} = 1$ is much worse than other schemes. As such, partial CQI feedback brings substantial sum rate gains relative to 1-CQI feedback.

Fig. 8 depicts the exact sum rate for ideal CQI feedback versus P_{s}/σ^2 for different M_{FB}s. We observe that the rate gap between the curves almost keeps as a constant in the high SNR regime. Importantly, increasing P_{S}/σ^2 does not decrease the rate gap between 1-CQI feedback with $M_{\text{FB}} = 1$ and other schemes. Based on Figs. 7 and 8, we conclude that when downlink resources are limited, the performance of MRN can be improved by increasing M_{FB}. Particularly, the value of M_{FB} needs to be carefully determined such that a comparable

performance to the full feedback scheme is achieved without consuming excessive feedback overhead.

C. Impact of Quantization

Fig. 9 compares the exact sum rate for ideal CQI feedback with the exact sum rate for quantized CQI feedback versus K for different number of quantization levels. We also plot the asymptotic sum rate for quantized CQI feedback. Without loss of generality, in this figure we consider the uniform quantization scheme. We first observe that the asymptotic curves accurately approximate the exact curves when K becomes large, which demonstrates the validity of our asymptotic result. We then observe that ideal CQI feedback achieves a higher sum rate relative to quantized CQI feedback. We also observe that the sum rate for quantized CQI feedback approaches that for ideal CQI feedback when L increases. This is due to the fact that a larger L allows more CQI feedback from the destinations, which increases the accuracy of CQI and in turn leads to a higher sum rate.

To investigate the sum rate loss caused by quantization, we define the sum rate gap between ideal CQI and quantized CQI as

$$G = R_{\text{sum}}^{(\text{I})} - R_{\text{sum}}^{(\text{Q})}. \tag{48}$$

In the regime of large K, we approximate (48) as

$$\begin{aligned} G &\approx \hat{R}_{\text{sum}}^{(\text{I})} - R_{\text{sum}}^{(\text{Q})} \\ &= \frac{1}{2K}\sum_{k=1}^{K}\sum_{\mu=1}^{K} \Xi\left[\frac{M_{\text{FB}}}{M_{\text{RB}}}, K, \mu\right](I_1(K; m_0, m_k, \beta_0, \beta_k). \\ &\quad - I_2(\mu; \xi_1, \cdots, \xi_L)). \end{aligned} \tag{49}$$

In the special case of full feedback, i.e., $M_{\text{FB}} = M_{\text{RB}}$, (49) can be further simplified as

$$G = \frac{1}{2K}\sum_{k=1}^{K}(I_1(K; m_0, m_k, \beta_0, \beta_k) - I_2(K; \xi_1, \cdots, \xi_L)). \tag{50}$$

We highlight from (50) that this gap no longer depends on M_{RB} in the case of full feedback. This is due to the fact that scheduling outage does not occur in the network when $M_{\text{FB}} = M_{\text{RB}}$.

Fig. 10 depicts G versus L for different number of destinations. Fig. 11 depicts G versus L for different number of feedback CQIs. In both figures the dash-dot curves are obtained from (49) and the marks are obtained from simulation results. We first observe from Figs. 10 and 11 that G decreases when$L$ increases. This implies that the sum rate of quantized CQIapproaches that of ideal CQI when the larger number of bits are usedfor feedback. We then observe from Fig. 10 that G increases when K increases. We further observe from Fig. 11 that G increases when M_{FB} increases. These observations are due to the fact that S receives more quantized CQIs when K or M_{FB} increases. When more quantized CQIs are fed back, the level of quantization noise increases, leading to a degraded sum rate.

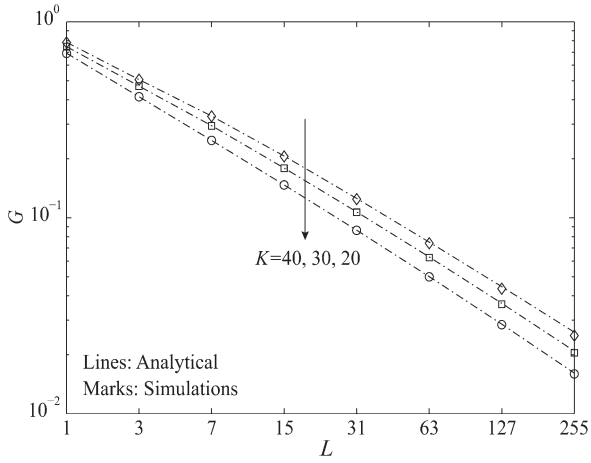

Fig. 10. G versus L for $P_{\text{S}}/\sigma^2 = P_{\text{R}}/\sigma^2 = 10$ dB, $M_{\text{RB}} = 10$, $M_{\text{FB}} = 10$, $m = 2$, and $d_{\text{S,R}} = d_{\text{R,D}_k} = 1$, $k \in \{1, \cdots, K\}$.

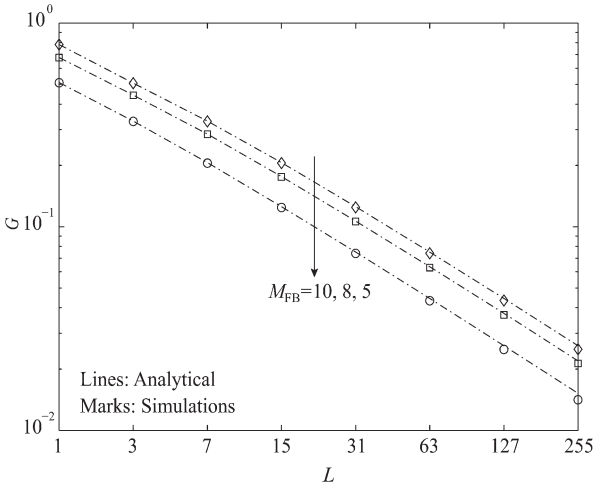

Fig. 11. G versus L for $P_{\text{S}}/\sigma^2 = P_{\text{R}}/\sigma^2 = 10$ dB, $M_{\text{RB}} = 10$, $K = 40$, $m = 2$, and $d_{\text{S,R}} = d_{\text{R,D}_k} = 1$, $k \in \{1, \cdots, K\}$.

V. Conclusion

We proposed and analyzed a new partial feedback scheme withopportunistic scheduling in multiuser relay networks. Considering the highly versatile Nakagami-m fading, we derived new exact closed-form expressions for the sum rate for two scenarios, namely, ideal CQI feedback and quantized CQI feedback. Using these expressions, we examined the impact of network configurations and channel parameters on the sum rate via numerical results. We also derived an asymptotic expression for the sum rate for ideal CQI feedback. We demonstrated that a more severe scattering environment with lower m reduces the sum rate for a small K, but improves the sum rate for a large K. We also demonstrated that a higher M_{RB} worsens the sum rate for a fixed M_{FB}, and a higher M_{FB} increases the sum rate for a fixed M_{RB}. Furthermore, we demonstrated that the sum rate gap between ideal CQI feedback and quantized CQI feedback decreases as the quantization level increases, while this gap increases as K or M_{FB} increases.

APPENDIX A
PROOF OF EQUATION (25)

To derive $I_1(N; m_0, m_k, \beta_0, \beta_k)$ in (25), we first present *Lemma 1* as follows.

Lemma 1: We decompose $d(F_{\tilde{\gamma}_k}(\gamma))^N, N \in \mathbb{N}^+$, as

$$d\left(F_{\tilde{\gamma}_k}(\gamma)\right)^N = \frac{N\gamma^{\hat{m}_k-1}}{(\hat{m}_k-1)!}\sum_{n=0}^{N-1}\sum_{\ell=0}^{\tilde{m}_{k,n}}\binom{N-1}{n}(-1)^n w_{k,n,\ell} \times \gamma^{\ell} e^{-(n+1)(\beta_0+\beta_k)\gamma}d\gamma, \quad (51)$$

where $\hat{m}_k = \min\{m_0, m_k\}$, $\tilde{m}_{k,n} = n(m_0+m_k-2)+\check{m}_k-1$ with $\check{m}_k = \max\{m_0, m_k\}$.

Proof: Note that $d(F_{\tilde{\gamma}_k}(\gamma))^N$ is expressed as

$$d\left(F_{\tilde{\gamma}_k}(\gamma)\right)^N = N\left(F_{\tilde{\gamma}_k}(\gamma)\right)^{N-1} f_{\tilde{\gamma}_k}(\gamma)d\gamma. \quad (52)$$

With the aid of [33, Eq. (8.352.1)], the CDF of $\gamma_{u,b}$ is rewritten as

$$F_{\gamma_{u,b}}(\gamma) = 1 - e^{-\beta_u\gamma}\sum_{\lambda_i=0}^{\epsilon_i-1}\frac{(\beta_u\gamma)^{\epsilon_i}}{\epsilon_i!}, \quad (53)$$

and $f_{\tilde{\gamma}_k}(\gamma)$ in (8) is rewritten as

$$\begin{aligned} f_{\tilde{\gamma}_k}(\gamma) &= \frac{\beta_k^{m_k}}{\Gamma(m_k)}\gamma^{m_k-1}e^{-(\beta_0+\beta_k)\gamma}\sum_{\epsilon_0=0}^{m_0-1}\frac{(\beta_0\gamma)^{\epsilon_0}}{\epsilon_0!} \\ &\quad + \frac{\beta_0^{m_0}}{\Gamma(m_0)}\gamma^{m_0-1}e^{-(\beta_0+\beta_k)\gamma}\sum_{\epsilon_k=0}^{m_k-1}\frac{(\beta_k\gamma)^{\epsilon_k}}{\epsilon_k!} \\ &= \frac{e^{-(\beta_0+\beta_k)\gamma}}{\Gamma(\hat{m}_k)}\gamma^{\hat{m}_k-1}\sum_{\epsilon=0}^{\check{m}_k-1}a_\epsilon\gamma^{\epsilon}. \end{aligned} \quad (54)$$

Substituting (53) into (7), we obtain

$$\begin{aligned} F_{\tilde{\gamma}_k}(\gamma) &= 1 - e^{-(\beta_0+\beta_k)\gamma}\left(\sum_{\epsilon_0=0}^{m_0-1}\frac{(\beta_0\gamma)^{\epsilon_0}}{\epsilon_0!}\right)\left(\sum_{\epsilon_k=0}^{m_k-1}\frac{(\beta_k\gamma)^{\epsilon_k}}{\epsilon_k!}\right) \\ &= 1 - e^{-(\beta_0+\beta_k)\gamma}\sum_{\omega=0}^{m_0+m_k-2}c_\omega\gamma^{\omega}, \end{aligned} \quad (55)$$

where c_ω is the $(\omega+1)$th entry of $\mathbf{c} = \mathbf{c}_1 * \mathbf{c}_2$. Based on (55), $(F_{\tilde{\gamma}_k}(\gamma))^{N-1}$ is rewritten as

$$\begin{aligned} &\left(F_{\tilde{\gamma}_k}(\gamma)\right)^{N-1} \\ &= \sum_{n=0}^{N-1}\binom{N-1}{n}(-1)^n e^{-n(\beta_0+\beta_k)\gamma}\left(\sum_{\omega=0}^{m_0+m_k-2}c_\omega\gamma^{\omega}\right)^n \\ &= \sum_{n=0}^{N-1}\binom{N-1}{n}(-1)^n e^{-n(\beta_0+\beta_k)\gamma}\left(\sum_{\omega=0}^{n(m_0+m_k-2)}g_{n,\upsilon}\gamma^{\upsilon}\right), \end{aligned} \quad (56)$$

where $g_{n,\upsilon}$ is the $(\upsilon+1)$th entry of $\mathbf{g}_n$ with $\mathbf{g}_n = \underbrace{\mathbf{c} * \mathbf{c} * \cdots * \mathbf{c}}_{n}$.

Substituting (54) and (56) into (52), we obtain

$$\begin{aligned} &d\left(F_{\tilde{\gamma}_k}(\gamma)\right)^N \\ &= N\left[\sum_{n=0}^{N-1}\binom{N-1}{n}(-1)^n e^{-n(\beta_0+\beta_k)\gamma}\sum_{\upsilon=0}^{n(m_0+m_k-2)}g_{n,\upsilon}\gamma^{\upsilon}\right] \\ &\quad \times\left[\frac{e^{-(\beta_0+\beta_k)\gamma}}{\Gamma(\hat{m}_k)}\gamma^{\hat{m}_k-1}\sum_{\epsilon=0}^{\check{m}_k-1}a_\epsilon\gamma^{\epsilon}\right]d\gamma \\ &= N\frac{\gamma^{\hat{m}_k-1}}{\Gamma(\hat{m}_k)}\sum_{n=0}^{N-1}\binom{N-1}{n}(-1)^n e^{-(n+1)(\beta_0+\beta_k)\gamma} \\ &\quad \times\left[\left(\sum_{\upsilon=0}^{n(m_0+m_k-2)}g_{n,\upsilon}\gamma^{\upsilon}\right)\left(\sum_{\epsilon=0}^{\check{m}_k-1}a_\epsilon\gamma^{\epsilon}\right)\right]d\gamma. \end{aligned} \quad (57)$$

Expanding the product of $\sum_{\upsilon=0}^{n(m_0+m_k-2)}g_{n,\upsilon}\gamma^{\upsilon}$ and $\sum_{\epsilon=0}^{\check{m}_k-1}a_\epsilon\gamma^{\epsilon}$ in (57), we derive the desired result in (51). ■

Substituting (51) into (24), we obtain

$$\begin{aligned} &I_1(N; m_0, m_k, \beta_0, \beta_k) \\ &= \frac{N}{(\hat{m}_k-1)!}\sum_{n=0}^{N-1}\sum_{\ell=0}^{\tilde{m}_{k,n}}\binom{N-1}{n}(-1)^n w_{k,n,\ell} \\ &\quad \times\int_0^{\infty}\log_2(1+\gamma)\gamma^{\hat{m}_k+\ell-1}e^{-(n+1)(\beta_0+\beta_k)\gamma}d\gamma. \end{aligned} \quad (58)$$

Using [43, Eq. (78)] to calculate the integral involved in (58), we obtain $I_1(N; m_0, m_k, \beta_0, \beta_k)$ as shown in (25), which completes the proof.

APPENDIX B
PROOF OF $F_{Y_{k,b}^{(\mathrm{Q})}}(\xi_l) = F_{Y_{k,b}^{(\mathrm{I})}}(\xi_l)$

Based on (36), we obtain

$$\begin{cases} \Pr\left(Y_{k,b}^{(\mathrm{Q})} = \xi_L\rho_{\mathrm{R}}\right) = & 1 - F_{Y_{k,b}^{(\mathrm{I})}}(\xi_l) \\ \Pr\left(Y_{k,b}^{(\mathrm{Q})} = \xi_{L-1}\rho_{\mathrm{R}}\right) = & F_{Y_{k,b}^{(\mathrm{I})}}(\xi_L) - F_{Y_{k,b}^{(\mathrm{I})}}(\xi_{L-1}) \\ & \vdots \\ \Pr\left(Y_{k,b}^{(\mathrm{Q})} = \xi_l\rho_{\mathrm{R}}\right) = & F_{Y_{k,b}^{(\mathrm{I})}}(\xi_{l+1}) - F_{Y_{k,b}^{(\mathrm{I})}}(\xi_l) \\ & \vdots \\ \Pr\left(Y_{k,b}^{(\mathrm{Q})} = \xi_2\rho_{\mathrm{R}}\right) = & F_{Y_{k,b}^{(\mathrm{I})}}(\xi_3) - F_{Y_{k,b}^{(\mathrm{I})}}(\xi_2) \\ \Pr\left(Y_{k,b}^{(\mathrm{Q})} = \xi_1\rho_{\mathrm{R}}\right) = & F_{Y_{k,b}^{(\mathrm{I})}}(\xi_2) - F_{Y_{k,b}^{(\mathrm{I})}}(\xi_1). \end{cases} \quad (59)$$

We then note that $F_{Y_{k,b}^{(\mathrm{Q})}}(\xi_l)$ can be derived as

$$\begin{aligned} F_{Y_{k,b}^{(\mathrm{Q})}}(\xi_l) &= \Pr\left(Y_{k,b}^{(\mathrm{Q})} < \xi_l\rho_{\mathrm{R}}\right) \\ &= \sum_{i=1}^{l-1}\Pr\left(Y_{k,b}^{(\mathrm{Q})} = \xi_i\rho_{\mathrm{R}}\right) \\ &= F_{Y_{k,b}^{(\mathrm{I})}}(\xi_l), \end{aligned} \quad (60)$$

which completes the proof.

REFERENCES

[1] D. N. C. Tse, "Optimal power allocation over parallel Gaussian broadcast channels," in *Proc. IEEE ISIT*, Jun. 1997, p. 27.

[2] L. Yang and M.-S. Alouini, "Performance analysis of multiuser selection diversity," *IEEE Trans. Veh. Technol.*, vol. 55, no. 6, pp. 1848–1861, Nov. 2006.

[3] X. Liu, E. K. Chong, and N. B. Shroff, "A framework for opportunistic scheduling in wireless networks," *Comput. Netw.*, vol. 41, no. 4, pp. 451–474, Mar. 2003.

[4] P. Bender *et al.*, "CDMA/HDR: A bandwidth efficient high speed wireless data service for nomadic users," *IEEE Commun. Mag.*, vol. 38, no. 7, pp. 70–77, Jul. 2000.

[5] K. I. Pedersen, P. E. Mogensen, and T. E. Kolding, "Overview of QoS options for HSDPA," *IEEE Commun. Mag.*, vol. 44, no. 7, pp. 100–105, Sep. 2006.

[6] V. Hassel, D. Gesbert, M.-S. Alouini, and G. E. Oien, "A threshold-based channel state feedback algorithm for modern cellular systems," *IEEE Trans. Wireless Commun.*, vol. 6, no. 7, pp. 2422–2426, Jul. 2007.

[7] J. W. So and J. Cioffi, "Capacity and fairness in multiuser diversity systems with opportunistic feedback," *IEEE Commun. Lett.*, vol. 12, no. 9, pp. 648–650, Sep. 2008.

[8] T. Tang, R. W. Heath, S. Cho, and S. Yun, "Opportunistic feedback for multiuser MIMO systems with linear receivers," *IEEE Trans. Commun.*, vol. 55, no. 5, pp. 1020–1032, May 2007.

[9] R. Agarwal, V. Majjigi, Z. Han, R. Vannithamby, and J. Cioffi, "Low complexity resource allocation with opportunistic feedback over downlink OFDMA networks," *IEEE J. Sel. Areas Commun.*, vol. 26, no. 8, pp. 1462–1472, Oct. 2008.

[10] J. Chen, R. Berry, and M. Honig, "Limited feedback schemes for downlink OFDMA based on sub-channel groups," *IEEE J. Sel. Areas Commun.*, vol. 26, no. 8, pp. 1451–1461, Oct. 2008.

[11] J. Leinonen, J. Hamalainen, and M. Juntti, "Performance analysis of downlink OFDMA resource allocation with limited feedback," *IEEE Trans. Wireless Commun.*, vol. 8, no. 6, pp. 2927–2937, Jun. 2009.

[12] S. Sanayei and A. Nosratinia, "Opportunistic downlink transmission with limited feedback," *IEEE Trans. Inf. Theory*, vol. 53, no. 11, pp. 4363–4372, Nov. 2007.

[13] D. Gesbert and M.-S. Alouini, "How much feedback is multi-User diversity really worth?" in *Proc. IEEE ICC*, Jun. 2004, pp. 234–238.

[14] Y. J. Choi and S. Bahk, "Partial channel feedback schemes maximizing overall efficiency in wireless networks," *IEEE Trans. Wireless Commun.*, vol. 7, no. 4, pp. 1306–1314, Apr. 2008.

[15] S. Hur and B. D. Rao, "Sum rate analysis of a reduced feedback OFDMA downlink system employing joint scheduling and diversity," *IEEE Trans. Signal Process.*, vol. 60, no. 2, pp. 862–876, Feb. 2012.

[16] Y. Huang and B. D. Rao, "Sum rate analysis of one-pico-inside OFDMA network with opportunistic scheduling and selective feedback," *IEEE Signal Process. Lett.*, vol. 19, no. 7, pp. 383–386, Jul. 2012.

[17] "Evolved Universal Terrestrial Radio Access (E-UTRA); Relay architectures for E-UTRA (LTE-Advanced)," 3rd Generation Partnership Project, Sophia Antipolis Cedex, France, 3GPP TR 36.806, v9.0.0, 2010.

[18] "LTE physical layer—General description (Release 10)," 3rd Generation Partnership Project, Sophia Antipolis Cedex, France, 3GPP TS 36.201, v10.0.0, 2010.

[19] Y. Yang, H. Hu, J. Xu, and G. Mao, "Relay technologies for WiMax and LTE-advanced mobile systems," *IEEE Commun. Mag.*, vol. 47, no. 10, pp. 100–105, Oct. 2009.

[20] J. Sydir and R. Taori, "An evolved cellular system architecture incorporating relay stations," *IEEE Commun. Mag.*, vol. 47, no. 6, pp. 115–121, Jun. 2009.

[21] W. Nam, W. Chang, S. Chung, and Y. Lee, "Transmit optimization for relay-based cellular OFDMA systems," in *Proc. IEEE ICC*, Jun. 2007, pp. 5714–5719.

[22] B. Kim and J. Lee, "Joint opportunistic subchannel and power scheduling for relay-based OFDMA networks with scheduling at relay stations," *IEEE Trans. Veh. Technol.*, vol. 59, no. 5, pp. 138–2148, Jun. 2010.

[23] A. Sharifian, P. Djukic, H. Yanikomeroglu, and J. Zhang, "Generalized proportionally fair scheduling for multi-user amplify-and-forward relay networks," in *Proc. IEEE 71st VTC—Spring*, May 2010, pp. 1–5.

[24] Y. Lin and W. Yu, "Fair scheduling and resource allocation for wireless cellular network with shared relays," *IEEE J. Sel. Areas Commun.*, vol. 30, no. 8, pp. 1530–1540, Sep. 2012.

[25] A. Zafar, M. Shaqfeh, M.-S. Alouini, and H. Alnuweiri, "Exploiting multi-user diversity and multi-hop diversity in dual-hop broadcast channels," *IEEE Trans. Wireless Commun.*, vol. 12, no. 7, pp. 3314–3325, Jul. 2013.

[26] N. Yang, P. L. Yeoh, M. Elkashlan, J. Yuan, and I. B. Collings, "On the SER of distributed TAS/MRC in MIMO multiuser relay networks," in *Proc. IEEE 73rd VTC—Spring*, May 2011, pp. 1–5.

[27] N. Yang, M. Elkashlan, and J. Yuan, "Outage probability of multiuser relay networks in Nakagami-*m* fading channels," *IEEE Trans. Veh. Technol.*, vol. 59, no. 5, pp. 2120–2132, Jun. 2010.

[28] N. Yang, M. Elkashlan, and J. Yuan, "Impact of opportunistic scheduling on cooperative dual-hop relay networks," *IEEE Trans. Commun.*, vol. 59, no. 3, pp. 689–694, Mar. 2011.

[29] N. Yang, P. L. Yeoh, M. Elkashlan, J. Yuan, and I. B. Collings, "Cascaded TAS/MRC in MIMO multiuser relay networks," *IEEE Trans. Wireless Commun.*, vol. 11, no. 10. pp. 3829–3839, Oct. 2012.

[30] M. Nakagami, "The *m*-distribution-A general formula of intensity distribution of rapid fading," in *Statistical Methods in Radio Wave Propagation*, W. G. Hoffman Ed. Oxford, U.K.: Pergamon, 1960, pp. 3–36.

[31] H. Suzuki, "A statistical model for urban radio propagation," *IEEE Trans. Commun.*, vol. COM-25, no. 7, pp. 673–680, Jul. 1977.

[32] A. U. Sheikh, M. Handforth, and M. Abdi, "Indoor mobile radio channel at 946 MHz: Measurements and modeling," in *Proc. IEEE 43rd VTC—Spring*, May 1993, pp. 73–76.

[33] I. S. Gradshteyn and I. M. Ryzhik, *Table of Integrals, Series, and Products*, 7th ed. San Diego, CA, USA: Academic, 2007.

[34] C.-J. Chen and L.-C. Wang, "A unified capacity analysis for wireless systems with joint multiuser scheduling and antenna diversity in Nakagami fading channels," *IEEE Trans. Commun.*, vol. 54, no. 3, pp. 469–478, Mar. 2006.

[35] Y. Lu, N. Yang, H. Dai, and X. Wang, "Opportunistic decode-and-forward relaying with beamforming in two-wave with diffuse power fading channels," *IEEE Trans. Veh. Technol.*, vol. 61, no. 7, pp. 3050–3060, Sep. 2012.

[36] H. A. David and H. N. Nagaraja, *Order Statistics*, 3rd ed. New York, NY, USA: Wiley, 2004.

[37] A. Kuhne, "Transmit antenna selection and OSTBC in adaptive multiuser OFDMA systems with different user priorities and imperfect CQI," in *Proc. Int. ITG WSA*, Feb. 2010, pp. 218–225.

[38] J. A. Gubner, *Probability and Random Processes for Electrical and Computer Engineers*. Cambridge Univ. Press: New York, NY, USA, 2006, ch. 12.

[39] A. Leon-Garcia, *Probability and Random Processes for Electrical Engineering*, 2nd ed. Cambridge, MA, USA: Addison-Wesley, 1994.

[40] M. Abramowitz and I. A. Stegun, *Handbook of Mathematical Functions with Formulas, Graphs, and Mathematical Tables*, 9th ed. New York, NY, USA: Dover, 1970.

[41] M.-S. Alouini and A. J. Goldsmith, "Capacity of Nakagami multipath fading channels," in *Proc. IEEE VTC—Spring*, May 1997, pp. 358–362.

[42] B. C. Jung, T. W. Ban, W. Choi, and D. K. Sung, "Capacity analysis of simple and opportunistic feedback schemes in OFDMA systems," in *Proc. IEEE ISCIT*, Oct. 2007, pp. 203–208.

[43] M.-S. Alouini and A. J. Goldsmith, "Capacity of Rayleigh fading channels under different adaptive transmission and diversity-combining techniques," *IEEE Trans. Veh. Technol.*, vol. 48, no. 4, pp. 1165–1181, Aug. 1999.

Yao Lu received the B.S. degree in electronic engineering from University of Electronic Science and Technology of China, China, in 2004, and the M.S. and Ph.D. degrees in electronic engineering from Beijing Institute of Technology, China, in 2006 and 2010, respectively. From 2010 to 2012, he worked as a Postdoctoral Research Fellow in the School of Information and Communication, Beijing University of Posts and Telecommunications, China. Since March 2012, he has been a Researcher with China Information Technology Designing and Consulting Institute of China Unicom. His general research interests include the areas of cooperative networks, MIMO systems, and self-organizing networks.

Nan Yang (S'09–M'11) received the B.S. degree in electronics from China Agricultural University, in 2005, and the M.S. and Ph.D. degrees in electronic engineering from the Beijing Institute of Technology, in 2007 and 2011, respectively. He is currently a Future Engineering Research Leadership Fellow and Lecturer in the Research School of Engineering, Australian National University. Prior to this, he was a Postdoctoral Research Fellow at the University of New South Wales (2012–2014) and a Postdoctoral Research Fellow at the Commonwealth Scientific and Industrial Research Organization (2010–2012). He received the IEEE ComSoc Asia-Pacific OutstandingYoung Researcher Award in 2014, the Exemplary Reviewer Certificate of the IEEE Wireless Communications Letters in 2014, the Exemplary Reviewer Certificate of the IEEE Communications Letters in 2012 and 2013, and the Best Paper Award at the IEEE 77th Vehicular Technology Conference in 2013. He serves as an editor of the TRANSACTIONS ON EMERGING TELECOMMUNICATIONS TECHNOLOGIES. His general research interests lie in the areas of communications theory and signal processing, with specific interests in collaborative networks, network security, massive multi-antenna systems, millimeter wave communications, and molecular communications.

Maged Elkashlan (M'06) received the Ph.D. degree in electrical engineering from the University of British Columbia, Canada, in 2006. From 2006 to 2007, he was with the Laboratory for Advanced Networking, University of British Columbia. From 2007 to 2011, he was with the Wireless and Networking Technologies Laboratory, Commonwealth Scientific and Industrial Research Organization (CSIRO), Australia. During this time, he held an adjunct appointment at University of Technology Sydney, Australia. In 2011, he joined the School of Electronic Engineering and Computer Science, Queen Mary University of London, U.K., as an Assistant Professor. He also holds visiting faculty appointments at the University of New South Wales, Australia, and Beijing University of Posts and Telecommunications, China. His research interests fall into the broad areas of communication theory, wireless communications, and statistical signal processing for distributed data processing, millimeter wave communications, cognitive radio, and wireless security.

Dr. Elkashlan currently serves as the Editor of the IEEE TRANSACTIONS ON WIRELESS COMMUNICATIONS, the IEEE TRANSACTIONS ON VEHICULAR TECHNOLOGY, and the IEEE COMMUNICATIONS LETTERS. He also serves as the Lead Guest Editor for the special issue on "Green Media: The Future of Wireless Multimedia Networks" of the *IEEE Wireless Communications Magazine*, Lead Guest Editor for the special issue on "Millimeter Wave Communications for 5 G" of the *IEEE Communications Magazine*, Guest Editor for the special issue on "Energy Harvesting Communications" of the *IEEE Communications Magazine*, and Guest Editor for the special issue on "Location Awareness for Radios and Networks" of the IEEE JOURNAL ON SELECTED AREAS IN COMMUNICATIONS. He received the Best Paper Award at the IEEE Vehicular Technology Conference (VTC-Spring) in 2013. He received the Exemplary Reviewer Certificate of the IEEE Communications Letters in 2012.

Jinhong Yuan (M'02–SM'11) received the B.E. and Ph.D. degrees in electronics engineering from the Beijing Institute of Technology, Beijing, China, in 1991 and 1997, respectively. From 1997 to 1999, he was a Research Fellow with the School of Electrical Engineering, University of Sydney, Sydney, Australia. In 2000, he joined the School of Electrical Engineering and Telecommunications, University of New South Wales, Sydney, Australia, where he is currently a Telecommunications Professor with the School. He has published two books, three book chapters, over 200 papers in telecommunications journals and conference proceedings, and 40 industrial reports. He is a co-inventor of one patent on MIMO systems and two patents on low-density-parity-check codes. He has co-authored three Best Paper Awards and one Best Poster Award, including the Best Paper Award from the IEEE Wireless Communications and Networking Conference, Cancun, Mexico, in 2011, and the Best Paper Award from the IEEE International Symposium on Wireless Communications Systems, Trondheim, Norway, in 2007. He is currently serving as an Associate Editor for the IEEE TRANSACTIONS ON COMMUNICATIONS. He serves as the IEEE NSW Chair of Joint Communications/Signal Processions/Ocean Engineering Chapter. His current research interests include error control coding and information theory, communication theory, and wireless communications.